

Generalized Modular Representation Framework for Process Synthesis

Katerina P. Papalexandri and Efstratios N. Pistikopoulos

Dept. of Chemical Engineering, Centre for Process Systems Engineering, Imperial College, London SW7 2BY, England

A generalized modeling framework for process synthesis alternatives is proposed, based on fundamental mass/heat-transfer principles. A multipurpose mass/heat-transfer module is introduced as the building block of the framework, whereas basic block-superstructure rules (such as splitting, mixing, and bypassing) are used to develop a systematic representation of process units and process structures, conventional or not. Process synthesis procedures are explored within this modeling framework, where synthesis alternatives are not postulated as process unit networks, but explored simultaneously without predefining synthesis schemes, as combinations of mass/heat-exchange stream matches. The representation potential of this framework is illustrated with examples from unit operations, whereas synthesis example problems are presented to show the broad range of process alternatives that can be modeled, identified, and optimized.

Introduction

Process synthesis has been developed in the past 25 years as the "act of determining the optimal interconnection of processing units as well as the optimal type and design of the units within a process system" (Nishida et al., 1981). In the beginning, work was focused on employing decomposition and heuristic rules in order to explore systematically synthesis alternatives and determine the optimal unit type and sequencing. Reviews on earlier developments can be found in Hendry et al. (1973) and Nishida et al. (1981). With the development of unit operations, on the one hand, that enabled a better understanding of processing tasks and mathematical programming, on the other, two basic approaches have been established to address the process synthesis problem: (1) hierarchical decomposition and evolutionary techniques, and (2) mathematical programming-based methods.

The superstructure representation of process alternatives has become a favorable approach since it provides a systematic basis for the evaluation and optimization of synthesis alternatives, especially with the evolution of mathematical programming techniques (Grossmann and Daichendt, 1994). Since process tasks are easier to model separately, most of the work in superstructure optimization has focused on the synthesis of subsystems, such as (1) *separation processes* (distillation sequences), (2) *heat-exchanger networks* (HEN), and (3) *reactor networks*.

Sharp-split and nonsharp-split separation of multicomponent mixtures has been modeled based on a column-building block, where separation tasks are preassigned to columns and emphasis was placed on column sequencing (Sargent and Gaminibandara, 1976; Floudas, 1987; Wehe and Westerberg, 1987; Floudas and Paules, 1988; Quesada and Grossmann, 1993). Heat integration possibilities have also been explored, coupling modeling concepts from distillation-sequence synthesis and heat-exchanger networks (Aggarwal and Floudas, 1992). While most of the research efforts were concentrated on separation of ideal mixtures, the synthesis of azeotropic distillation columns has also been studied based on geometric representation of residue curves (Knight and Doherty, 1989). More recently, for separation systems based on equilibrium, Rigg and Swaney (1994) proposed a unified-network representation, based on key thermodynamic states involved in the process. Countercurrent mass contactors are considered between pairs of states, pinched at one end. Sargent (1994) coupling concentration trajectory studies and state-task network representation proposed an evolutionary method of developing efficient separation structures, rather than superstructures, with the aim of handling azeotropic as well as ideal mixtures.

In the mature area of heat-exchanger networks, synthesis alternatives have been explored in a systematic manner through the development of HEN superstructures (Yee and Grossmann, 1990; Ciric and Floudas, 1991). Furthermore,

Correspondence concerning this article should be addressed to E. N. Pistikopoulos.

synthesis objectives have been extended beyond economics, to include operability aspects (Papalexandri and Pistikopoulos, 1994).

In reactor networks the objective has been to optimize the mixing pattern along with the operating conditions. Superstructure representations have been developed based on serial recycle reactor modules without bypass stream (Chitra and Govind, 1985), or comprising a recycle reactor, heat exchanger, fresh feed, and bypass stream (Achenie and Biegler, 1990), multifunctional continuous stirred-tank reactor (CSTR) modules interacting with heating/cooling blocks (Kokossis and Floudas, 1990; Kokossis and Floudas, 1994), or multi-component reactor modules that involve a segregated mixing zone and multiple zones of maximum mixedness (Balakrishna and Biegler, 1993).

Regarding the synthesis of total flowsheets, Kocis and Grossmann (1989) proposed a generalization of the flowsheet superstructure involving a set of interconnection nodes (splitters and mixers) and a set of unit nodes. The synthesis problem was formulated as a mixed-integer nonlinear optimization problem and OA/ER was employed for its solution (Duran and Grossmann, 1986; Kocis and Grossmann, 1987). Toward the same direction, Bagajewicz and Manousiouthakis (1992) introduced a state-space representation of synthesis alternatives, where one can distinguish a stream splitting/mixing block and a process unit block, where process units are either modeled through a superstructure operator, or synthesis tasks are explored employing pinch technology principles. In his review paper, Sirola (1995) employed means-end analysis and evolution techniques for systematically generating process synthesis alternatives. Starting from the initial state of raw materials toward the final product state, property differences are exploited in a hierarchical way to specify corrective tasks that should eliminate these differences (chemical reaction to change chemical identity, separation to change concentration and purity). Going beyond the evaluation stage of synthesis alternatives, Friedler et al. (1993) established a method for obtaining the "maximal" structure (superstructure) of all possible feasible alternatives for a process synthesis task, assuming a given set of process units to be considered.

However, a synthesis of entire flowsheets to date has been governed by an implicit assignment of processing tasks to processing equipment through a prepostulation of a set of unit operations within a superstructure realization of synthesis alternatives. Hence, the derived flowsheets are limited by typical flowsheet patterns that follow more or less the traditional hierarchical design guidelines. Hybrid process units and nonconventional process structures that have recently proved to be favorable in the industry, are only studied within an algorithmic superstructure-based approach when prepostulated (Ciric and Gu, 1994). The synthesis framework proposed in this article overcomes this limitation by employing fundamental mass/heat-transfer principles within a superstructure environment that exploits modeling concepts from the well-defined HEN problem.

Problem Statement

The synthesis problem addressed in this article can be stated as follows:

- A set of existing process streams to be used as raw materials, their flow rates, supply temperatures, and compositions.
- A set of desired products and specifications on their flow rates, outlet temperatures, and compositions.
- Available heat and/or mass utility streams, such as steam, cooling water, and active carbon, specifications on their availability (flow rate bounds), supply temperatures, and compositions.
- Physical property and cost data.

Then, *the objective* is to synthesize a process network, consisting of process units, such as distillation columns, reactors, and reactive distillations (nonequilibrium or not), that is able to satisfy the process specifications on the desired products and availability of utilities, optimizing a performance criterion, usually of economic nature (e.g., operating or total annualized cost).

It is assumed that the available technology for the production of the desired products is known, for example, the chemistry (kinetics, intermediates, byproducts), and solvents with increased solubilities. If for example aromatic hydrocarbons are to be recovered from an aromatic/paraffinic/naphthenic mixture, a number of extractive solvents, such as dimethylformamide (DMF) or *N*-methylpyrrolidone, are given.

In the sequel, a multipurpose mass/heat-transfer block will be introduced, characterized by mass- and heat-transfer phenomena. Their type and the substances that are involved define the process operation and the corresponding process unit.

Multipurpose Mass/Heat-Transfer Module

In general, a process operation is characterized by a set of mass- and heat-transfer phenomena, concerning mainly the mass transfer of a component from one substance or phase to another. For example:

- Distillation involves the mass and heat transfer between the vapor and liquid contacting phases of a mixture.
- Reaction involves the mass transfer (and heat transfer in terms of internal energy) from a reacting species to a product species.

Within the mass/heat-transfer context of process operations, one can distinguish components of interest, the concentration of which in one stream/phase increases, while in another stream/phase decreases. Thus, process operations may be viewed as sets of mass (and heat) exchangers between two properly defined sides/streams, a "rich" side (decreasing concentration) and a "lean" side (increasing concentration), following the terminology of mass-exchange networks (El-Halwagi and Manousiouthakis, 1989; Papalexandri et al., 1994). Furthermore, pure heat exchange between two streams, not directly or actively contacting, also is employed in process flowsheets.

Based on the mass/heat-transfer phenomena in process operations, a two-exchanger module is proposed to form the building block of a network superstructure of process alternatives (Figure 1). It comprises (1) a pure heat-exchange block, where the matching streams exchange only heat, not coming into active contact, and (2) a mass-and-heat exchange block, where mass-transfer direction (rich to lean side) is defined by a set of components of interest. Note that, although the pure heat-exchange block might in general be viewed as a special case of mass-and-heat exchanger, the dominant phe-

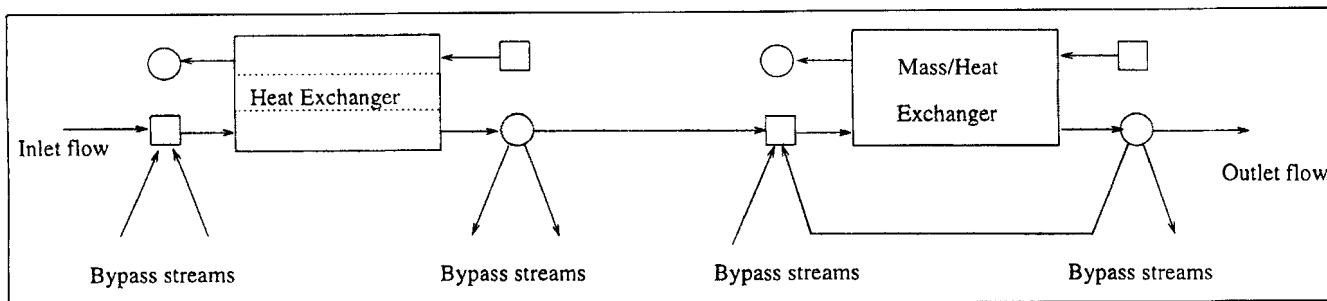


Figure 1. Multipurpose mass/heat-transfer module: ○ = splitter; □ = mixer.

nomenon is conductive heat transfer, while in the mass-and-heat-exchanger, block operation is defined by mass transfer/generation, which is based on different stream interaction.

The streams that appear in process operations to participate in mass/heat transfer are of different phase or of different (chemical) potential/composition. A *stream* is defined in this framework by its phase (vapor, liquid, organic, nonmiscible organic, etc.) and a qualitative indication of its composition (pure component, mixture of components, mixture rich in a specific component, etc.). For example, in the distillation of a binary mixture AB , the streams participating in the corresponding mass/heat transfer phenomena are a liquid and a vapor stream containing mostly A ($L_{A(B)}$ and $V_{A(B)}$, respectively) and a liquid and a vapor stream containing mostly B ($L_{(A)B}$ and $V_{(A)B}$). Alternatively, since composition-based differentiation, being qualitative, is conventional, we may say that in general we have a liquid mixture L_{AB} and a vapor mixture V_{AB} .

The mass and heat transfer in process operations take place between streams of different *potential*, which can be realized between different immiscible phases or in reactions (chemical potential), with the driving force for the mass transfer being a function of stream composition, temperature, and pressure. Hence, *mass/heat-transfer stream matches are considered between streams of different phase and between reagent/product streams when reactions are possible*. For example, in the distillation of a binary mixture AB , A (the most volatile component) is transferred from the liquid to the vapor phase of a mixture stream that contains mostly A (denoted as $L_{A(B)}$ and $V_{A(B)}$) and mixture that contains mostly B ($L_{(A)B} \rightarrow V_{(A)B}$); that is, mass/heat transfer is realized in stream matches $L_{A(B)}-V_{A(B)}$ and $L_{(A)B}-V_{(A)B}$. In both stream matches the concentration of the liquid stream in A is reduced; thus, the liquid streams act as the "rich" sides in mass transfer, whereas the vapor streams act as the "lean" sides. If reaction is also possible within AB toward a product C in the liquid phase, this could be realized as transfer of C from a stream that contains mostly A , B to a stream that has the potential to increase its concentration in C ("lean" in C), or contains mostly C ($L_{AB(C)} \rightarrow L_{(AB)C}$). In addition the following matches are considered: $L_{A(B)C}-V_{A(B)C}$, $L_{AB(C)}-V_{AB(C)}$, and $L_{(AB)C}-V_{(AB)C}$.

Based on the preceding definitions of streams and stream matches, within this framework, a network superstructure is developed [similar to the HEN hyperstructure proposed by Ciric and Floudas (1991)], assigning side mixers and splitters to each exchange block (see Figure 1) and considering all

stream interconnections between exchangers. An initial splitter is also considered for each existing stream and a final mixer for each possible existing, intermediate, and final stream.

An assumption is made, that at the mixers prior to each side of potential exchanger units and final mixers only stream flows of the *same* phase are merged. No phase change (flash operations) takes place at mixers. This can occur in the adjacent exchanger blocks; in this case, the exchanger inlet temperature is at most the mixture boiling point or at least the mixture dew point (in general, phase properties cannot take values beyond the phase critical property values, resulting in phase-defining constraints). The mixing assumption can be relaxed to cover the case of liquid-vapor streams (defining a separate stream type), for example, in the separation of a binary mixture AB we would have streams L_{AB} , V_{AB} , and LV_{AB} , where the latter is a mixed phase-stream (described accordingly).

The mass/heat-exchange superstructure is mainly described by mass and energy balances and thermodynamic constraints that ensure the existence of a driving force for mass/heat transfer. In particular:

Stream splitters at the network inlet of each existing stream and after the outlet of each exchanger side are described by mass balances for the total stream flows.

Stream mixers (at the inlet of each exchanger side and the network outlet of each stream) are described by mass balances for the total stream flows and each component separately, phase-defining constraints (depending on the phase of the stream defining the adjacent exchanger or product stream), and energy balances. For example, at the rich-side mixer of a match $L_{AB} \rightarrow V_{AB}$, we will have: total flow mass balance; mass balances for A and B ; energy balance; liquid-phase constraint of the type:

$$k_A x_A^{L_{AB},in} + k_B x_B^{L_{AB},in} \leq 1,$$

where k_A , k_B are phase equilibrium constraints for A and B at the temperature and pressure of L_{AB} at the inlet of the exchanger.

Pure heat exchangers are described by energy balances, phase-defining constraints at the exchanger outlets and driving-force constraints for heat transfer. The feasibility of heat transfer is ensured by a minimum positive temperature difference between the hot and the cold streams at the inlet and the outlet of the exchanger. In the case of vapor stream ex-

constraints, based on thermodynamic properties, are considered at the inlet (vapor phase) and the outlet (liquid phase) of the exchangers. Similarly, a heat exchanger $H - V(A)B$, where H is a hot stream or heating utility, acts as a reboiler when ensuring liquid phase at the mixer outlet prior to the exchanger and vapor phase at the exchanger outlet. When liquid-vapor mixture streams are considered ($LV_{(A)B}$, $LV_{A(B)}$). A partial reboiler and a partial condenser may be defined similarly ($H - LV_{(A)B}$ and $LV_{A(B)} - C$, respectively). In this case, thermodynamic properties are constrained within the limits that characterize a mixture stream, while boil-up and condensation ratios are variables. Phase-defining constraints refer to liquid-only, vapor-only, or vapor-liquid mixture, depending on the stream participating to the exchanger.

Bypass streams in Figure 2 are required from the lean side (in terms of A) of the lower part to the lean side of the upper part, from the rich side of the upper part to the rich side of the lower part, and from and to the condenser and the reboiler.

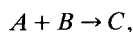
Note that for the case of binary mixtures the set of mass/heat-transfer modules comprising a conventional distillation column are similar to the set of mass exchangers proposed by Bagajewicz and Manousiouthakis (1992).

Complex columns with more than one feed and more than one product (side strippers, etc.) can be included as alternatives within the superstructure if multiple mass/heat exchange is considered between the liquid and the vapor streams of the upper and the lower parts of the column. In that case, the distillation column can be actually realized as a set of trays (corresponding to mass/heat-exchange modules), and more involved distillation models can be employed.

Homogeneous reaction

A homogeneous reactor can be realized as a mass/heat exchanger between the reagent mixture ("rich" in chemical potential, thus "rich" in reaction product, because it tends to "give away" C to the other stream product) and the reaction product mixture (where product concentration is increased, thus "lean" in reactor product).

Considering the reaction in the liquid phase



a reactor would result as a mass/heat exchanger between $L_{AB(C)}$ and $L_{(AB)C}$ (Figure 3). Such a block is modeled as described in the third section, with mass and energy balances, where the transferred quantity involves a

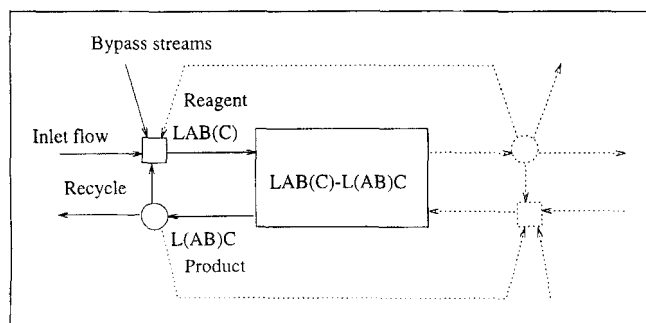


Figure 3. Homogeneous reactor.

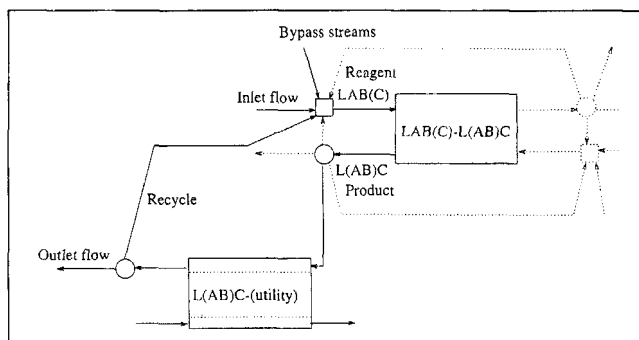


Figure 4. Jacketed homogeneous reactor.

reaction/generation term, and driving constraints based on kinetic constants. Since the reaction takes place in one phase, only one inlet and outlet must be present. A recycle stream would correspond to the bypass flow from the splitter after the lean-product outlet to the mixer prior to the rich-reagent inlet (see Figure 3). If the product stream exchanges heat with a cooling utility and there are no other bypass flows out of the lean side, a jacketed reactor may be realized (as in Figure 4).

One mass/heat exchanger representing a homogeneous reacting system would correspond to a CSTR, since implicitly we assume that the two mass/heat-exchanging streams are well mixed in order to define reaction kinetics. A plug-flow reactor (PFR) can be realized as a "battery" of mass/heat-exchanger units. Any other flow pattern and mixing scheme in a reactor will result through the interconnections of multiple mass/heat-exchange units of the same stream match. It must be noted that when only homogeneous reacting streams are considered, the mass/heat-exchange superstructure results in the nonisothermal reactor network superstructure proposed by Kokossis and Floudas (1994).

Two-phase reaction

A two-phase reaction can be realized as a mass/heat exchange between the two phases involved. The lean side is defined by the stream/phase, the concentration of which in the component of interest is increased. Both reactants and reaction products are considered present in each phase. Mass transfer between the two streams is now governed by chemical reaction and phase change, and is limited either by chemical or phase equilibrium. Since the two phases are immiscible, recycle streams are considered from each side splitter to the mixer prior to the same exchanger side, as illustrated in Figure 5.

Absorption/extraction

An absorber and/or an extractor is actually a mass/heat-exchange block, where a set of components (and heat possibly) are transferred between two immiscible phases (not of the same streams as in distillation). Mass transfer is governed by equilibrium of the two immiscible phases and distribution of the components of interest. Both units are represented by a single (or a set of, if detailed models are to be employed) mass/heat-exchange modules.

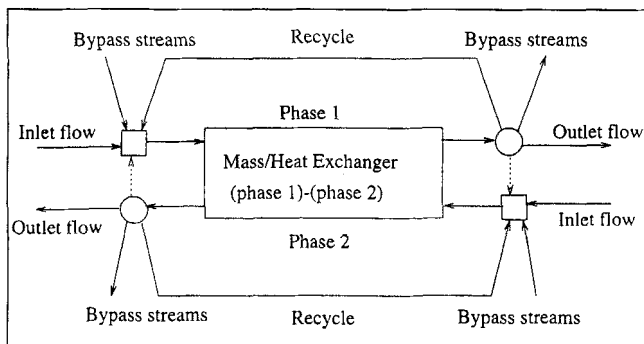


Figure 5. Two-phase reaction.

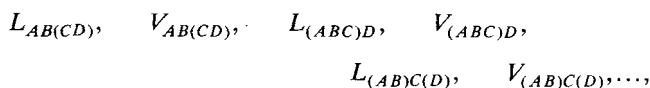
Reactive distillation

Reactive distillation can be realized similarly to conventional distillation, as a set of two or more mass/heat-exchange units between liquid-vapor streams. Note that in this case, the mass-exchanging streams correspond to the reacting systems, and those have already been accounted for as intermediate streams and alternative matches. Mass transfer is again governed by phase change and chemical reaction and is limited by phase and chemical equilibrium. Multiple feeds and products and side heating and/or cooling can be modeled by considering multiple mass/heat exchange between the liquid and the vapor of the reacting system.

Consider, for example, the production of C from A and B according to the following reversible reaction:



where D is the most volatile component, while C is the least volatile. Within the proposed modeling framework, based on the information given earlier, the following streams are considered:



or L_{ABCD} and V_{ABCD} in general, and all the possible matches in between them, that is, liquid-vapor matches of the same stream and liquid-liquid. Depending on the synthesis objective, alternative process structures featuring different operating conditions may result from the mass/heat-exchange superstructure module, for example, (1) the reaction taking place in the liquid phase up to equilibrium, and then A , B , and D are separated from C (see Figure 6), and (2) the reaction taking place in the liquid holdup of the trays of a distillation column, with D being removed to the vapor phase and chemical equilibrium shifted to the right (see Figure 7).

Note that *reactive adsorption* and/or *extraction* can be modeled using similar arguments.

Mass/Heat-Exchange Superstructure Representation

Mass/heat and pure heat exchangers are described by simple mass and energy balances, where mass and energy gener-

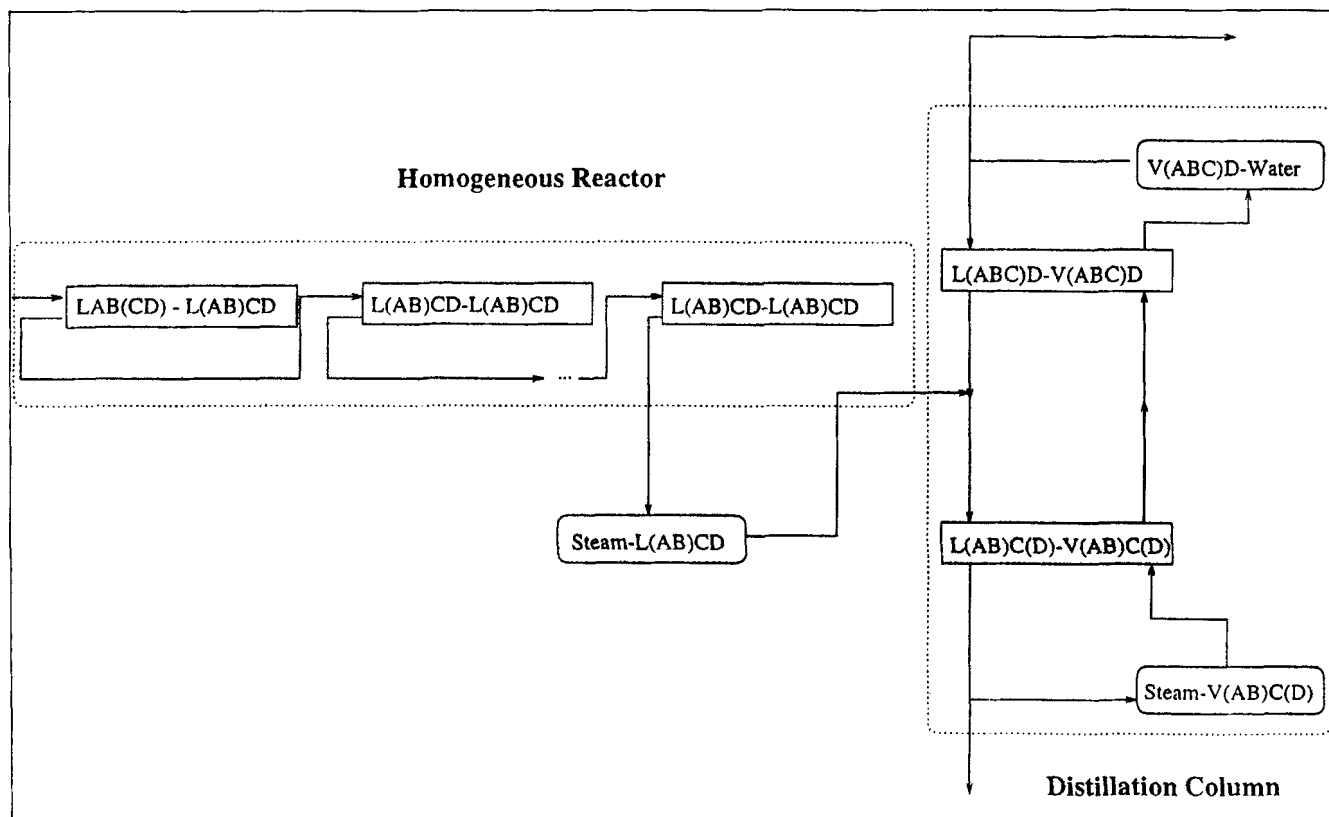


Figure 6. Production of C from A and B —alternative I.

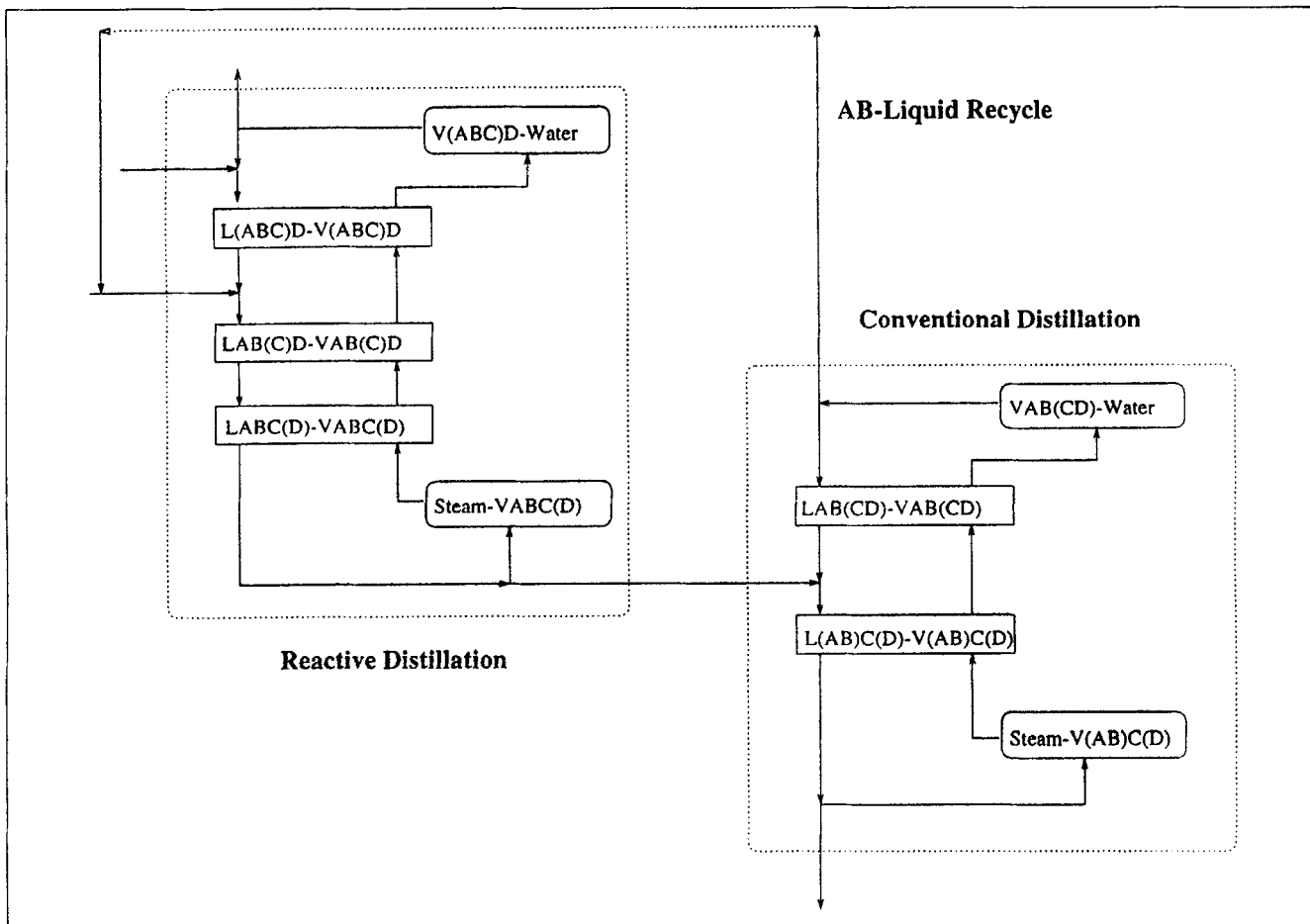


Figure 7. Production of C from A and B—alternative II.

ation and/or consumption are taken into consideration. Thus, the concepts of mass and heat transfer are broadened to include chemical reactions as well. Driving force constraints for mass transfer/reaction are considered at each end of the mass/heat-exchanger modules; similarly, for temperature approach constraints.

Mass transfer between immiscible phases is driven by ensuring a minimum approach (ϵ) of the system to equilibrium compositions. The same holds for mass transfer/generation/consumption when chemical reactions occur. Equilibrium may also be accounted for by setting $\epsilon \rightarrow 0$, that is, allowing the system a positive or zero driving force for mass transfer of each component of interest. Mass/heat exchangers featuring equilibrium compositions at one end ("active" driving force constraints) actually correspond to the "pinched" mass contactors of the Rigg-Swaney network representation (Rigg and Swaney, 1994).

When mass and/or heat transfer are governed by nonconvex driving force functions, constraining the two ends of a mass/heat exchanger may not suffice for a feasible mass/heat transfer throughout the exchanger. This could be overcome by discretization of the mass/heat exchange block, so that intermediate concentrations and temperatures are taken into account.

Nonideal behavior (e.g., azeotropic mixtures) has not been considered so far. In this case, in order to define the streams

that are present in the process, one may consider explicitly a potential azeotropic mixture as a separate phase and account for mass/heat exchange between possible entrainers or based on detailed thermophysical properties. *Nonconventional mass transfer*, for example, through membranes and biofilms, can be treated, considering each active contributor to mass transfer as a separate superstructure stream, contributing to separate mass/heat-exchange blocks. However, the applicability of mass/heat-exchange superstructure representation to nonideal separations is a subject of our current research work.

Synthesis Framework

The generalized mass/heat-transfer network superstructure can represent process alternatives systematically and in a unified way, as shown in the previous sections. A synthesis framework based on this representation scheme, where one would start from the synthesis with the aim to obtain an optimal process network, should involve (Figure 8):

- Construction of a stream superset, which includes *all the initial and desired process streams, as well as the intermediate streams that can result, based on the available knowledge on physicochemical trends*. In general, if limited information is available on intermediate streams, or many components are present, one mixture stream may be considered, containing

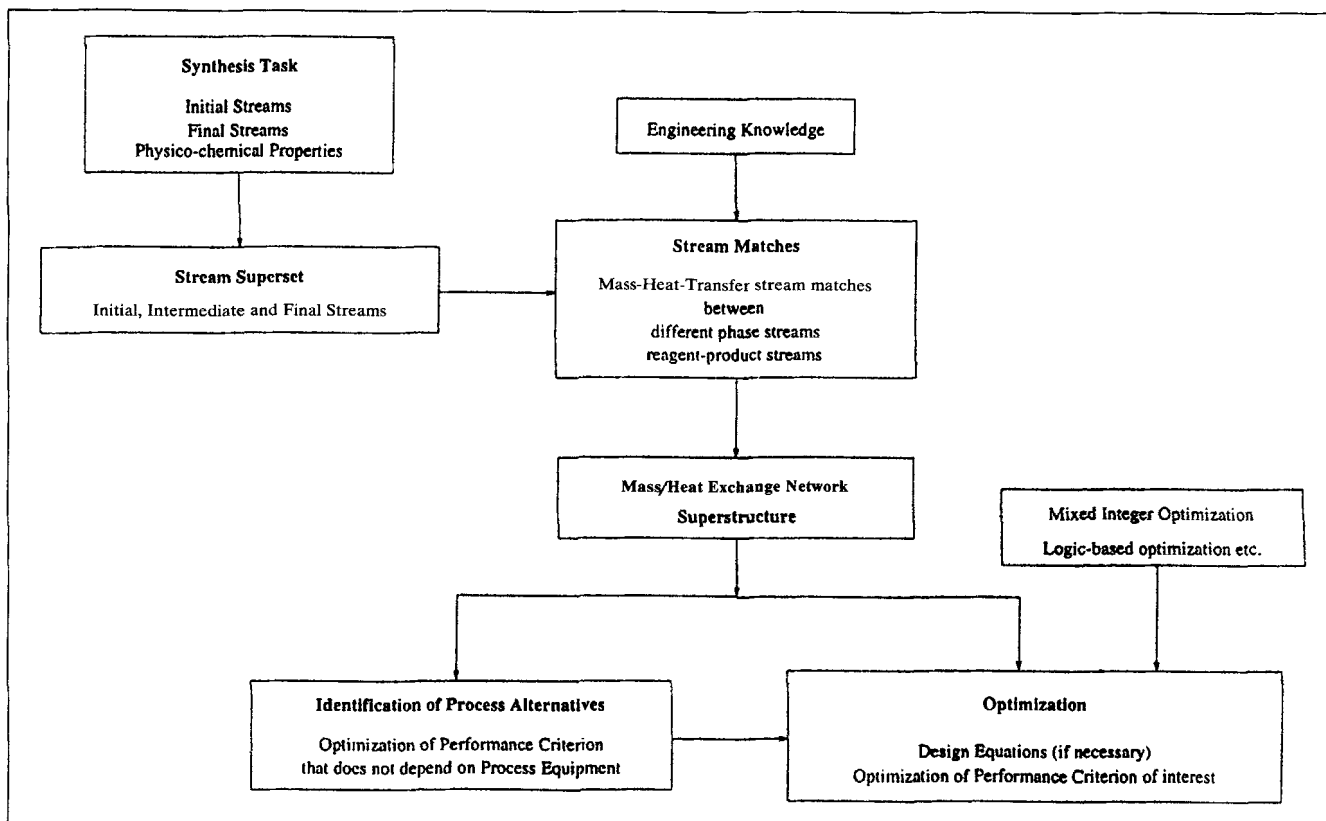
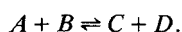


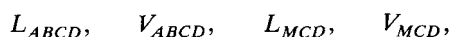
Figure 8. Synthesis framework.

all possible components (initial, intermediate, etc.) in all possible phases (including immiscible organic/inorganic phases). For example, consider the production of C (liquid) from A and B according to



We are given that $A > B > C > D$, in terms of relative volatility. Also M is miscible with C and D , but not with A and B .

Then the following streams may be considered: $ABC(D)$, $AB(CD)$, $A(BCD)$, $(AB)C(D)$, $(A)B(CD)$, $A(BCD)$; and $M(CD)$, $MC(D)$, $(MC)D$, $(M)C(D)$, in the liquid and vapor phase. Obviously, this would result in a large number of streams that are only different in composition by convention. Thus, instead, we may consider mixtures of miscible components in all phases, without any reference to their composition:

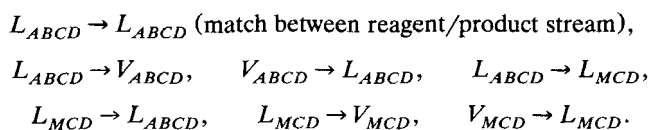


and any initial/existing and final/desired streams that cannot be considered instances of the intermediate streams just listed.

• Postulation of stream matches. Having defined process streams, all possible mass/heat-transfer matches are considered, defining the heat- and mass-transfer blocks in the superstructure. In many cases, mass/heat-transfer between streams may be realized in more than one way, for example, distillation or

reactive distillation. Thus, multiple mass/heat-transfer blocks are considered for each stream match. Engineering knowledge may be employed at this stage to exclude redundant stream matches and reduce problem dimensionality (*pre-screening*).

For example, in the production of C from A and B and for the case of mixture streams, we will have:



However, any vapor-vapor stream match would be meaningless since vapor streams are miscible and no reaction takes place in the vapor phase.

• Development of mass/heat-exchange network superstructure, considering all possible interconnections between the stream splitters and mixers of the stream superstructure of Figure 8.

• Optimization of the mass/heat-exchange superstructure. Conventional mixed integer nonlinear programming techniques or those coupled with logic-based optimization (Raman and Grossmann, 1993) can be employed for the solution of the resulting large-scale optimization problem.

Process synthesis is usually driven by the minimization of a cost function. Operating cost can be straightforwardly accounted for in the superstructure model, since it corresponds to raw material and utility consumption. Capital cost, how-

Table 1. Stream Data and Specifications for Acetone Recovery

Stream	Flow Rate kmol/h	Acetone Conc.	Temp. °C
Air mixture	316.29	0.01478	25
Air product	≥ 311.615	≤ 0.00029	25
Acetone product		≥ 0.99	25
Water effluent		≤ 0.05	25

Table 2. Utility Cost Data for Acetone Recovery

Utility	Annualized Cost
Scrubbing water	\$16.132/(kmol/h)yr
Cooling water	\$26.190/(kW)yr
Steam	\$137.27/(kW)yr
Water effluent	\$135,476.1/(kmol acetone/h)yr

ever, corresponds to equipment cost and cannot be readily incorporated, since process units are not considered. Capital cost can be approximated through "hybrid" capital cost functions based on operating conditions of processing tasks, for example, the cost of a distillation tray (liquid-vapor stream match) can be approximated based on the separation difficulty, which translates to inlet and outlet mole fractions and temperatures. Alternatively, one can explore at a first step process structures optimizing operating cost (or even total cost, where capital cost is approximated as before), while in a second step employ rigorous cost models for process units that may result from the optimization. In this case, each cost model should correspond to a certain arrangement of stream matches (see also example problems).

In the next section, the representation potential of the proposed framework is illustrated with examples from the areas of separations, heat-exchanger networks, and reactor-separation networks.

Examples

The mass/heat-exchange superstructure representation framework is employed in the following examples to explore alternative structures in a separation system, reactor-separation system, a potential hybrid production system, and heat integration networks, that cannot be handled with the conventional HEN synthesis techniques. The derived synthesis schemes are by no means proposed as economically global optima. However, they illustrate the representation potential of the proposed modular framework.

Example 1: acetone recovery from air mixture

The synthesis of an acetone recovery system at minimum total annualized cost (TAC) is of interest, where the air mixture is purified up to 98% and acetone is recovered in a product stream of at least 99% purity. Steam data and specifications are given in Table 1 (Douglas, 1988; Ciric and Jia, 1991).

Scrubbing water is available at 25°C for acetone removal from the air mixture. The desired acetone-rich product must be recovered at 25°C, while water effluent can be recycled in the process or discharged at 25°C with an upper acetone concentration of 5%, where a purification cost is introduced (Table 2).

Cooling water (CW) at 20°C and steam (S) at 182°C are available as cooling and heating utilities. Cost data for the utility consumption are given in Table 2.

The streams that can be present in the separation system, defining the *stream superset*, are air-acetone mixture, PA (it is assumed unlikely for PA to be present in the liquid phase, as well as to contain any water); acetone-rich product, liquid (LP) and vapor (VP); pure scrubbing water (W); water-rich product effluent, in the liquid (LW) and the vapor (VW) phase; cooling water (CW); and steam (S).

All possible mass/heat and pure heat-exchange matches are initially considered for acetone recovery (Figure 9). However, considering conventional conditions, not all exchangers are feasible or necessary (e.g., there is no reason in transferring acetone from LP to PA). Thus, a preliminary screening reduces significantly mass/heat and heat-exchanger possibilities. The mass/heat-exchange superstructure is developed, based on the resulting exchange matches of Figure 9, and all

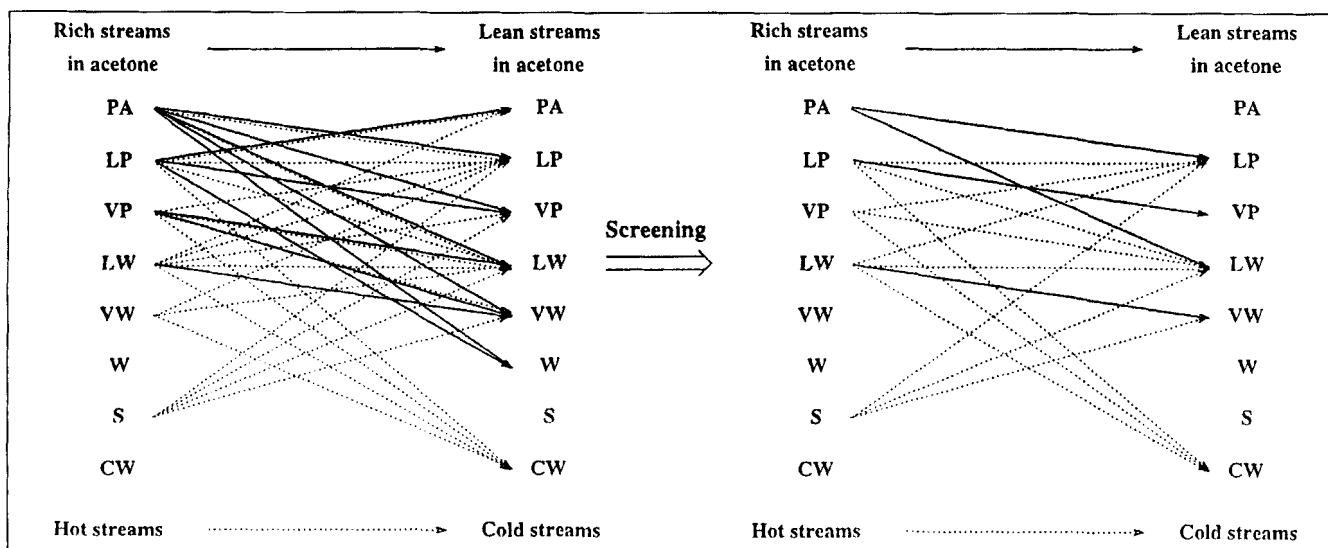


Figure 9. Mass/heat and heat-exchange matches for acetone recovery.

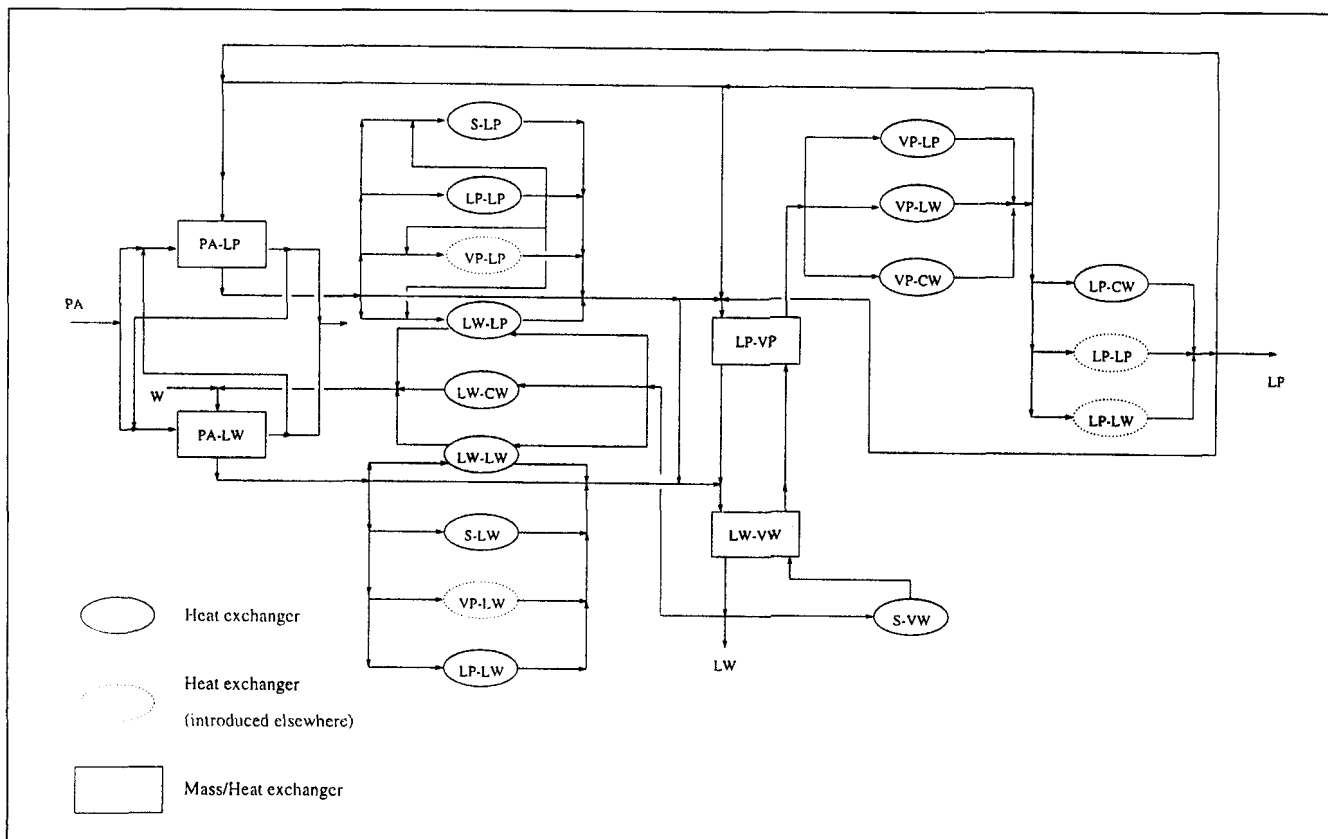


Figure 10. Superstructure alternatives for acetone recovery.

interconnections between exchangers are considered. Figure 10 presents some of the structural alternatives considered.

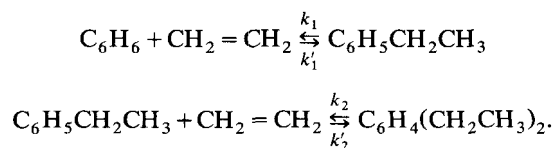
Mixed integer optimization techniques are employed for the superstructure optimization. The existence of each mass/heat- and pure heat-transfer block is denoted by a binary variable. Each block is described by mass/heat balances, considering acetone as the transferred component of interest. Operating cost is calculated based on utility consumption (see Table 2). Capital cost is simultaneously accounted for. Data are given in Table 3. The detailed superstructure model is described in Appendix A.

The mixed integer nonlinear programming (MINLP) synthesis model involved 848 rows, 544 continuous variables and 127 binary variables (from which only 16 are actually necessary, corresponding to mass/heat and heat-exchange blocks, while the rest aid the structural optimization; see Appendix A). The model was solved using generalized benders decomposition (GBD) through the modeling system GAMS (Brooke et al., 1988), in 6 GBD iterations, starting from the process structure illustrated in Figure 11. The proposed acetone recovery system is illustrated in Figure 12. It features an ab-

sorber, a distillation column, and a water recycle stream that is heat integrated with the distillation column feed, corresponding to a TAC = \$697,294/yr.

Example 2: production of ethylbenzene

In this example we study ethylbenzene production through alkylation of benzene. As reported by Kokossis and Floudas (1991), the process is an intermediate stage for the production of styrene using the direct hydrogenation method, and the reaction is carried out in the liquid phase, according to the following scheme:



Higher order alkylation products are not thought to form in significant amounts, and are ignored at this stage. Ethylene is assumed to be completely consumed by the reactions in the liquid phase, the rates of which are determined by first-order kinetics. The rate constants are taken equal for all reactions:

$$k_1 = k'_1 = k_2 = k'_2 = 0.4 \text{ h}^{-1}$$

Table 3. Capital Cost Data for Acetone Recovery

Equipment	Annualized Cost (\$/yr)
Heat exchanger	1,300 $A^{0.6}$
Absorber	3,400 $N_{tr}^{1.4}$
Distillation column	17,450 $N_{trays}^{1.4} V_{top}^{0.5}$

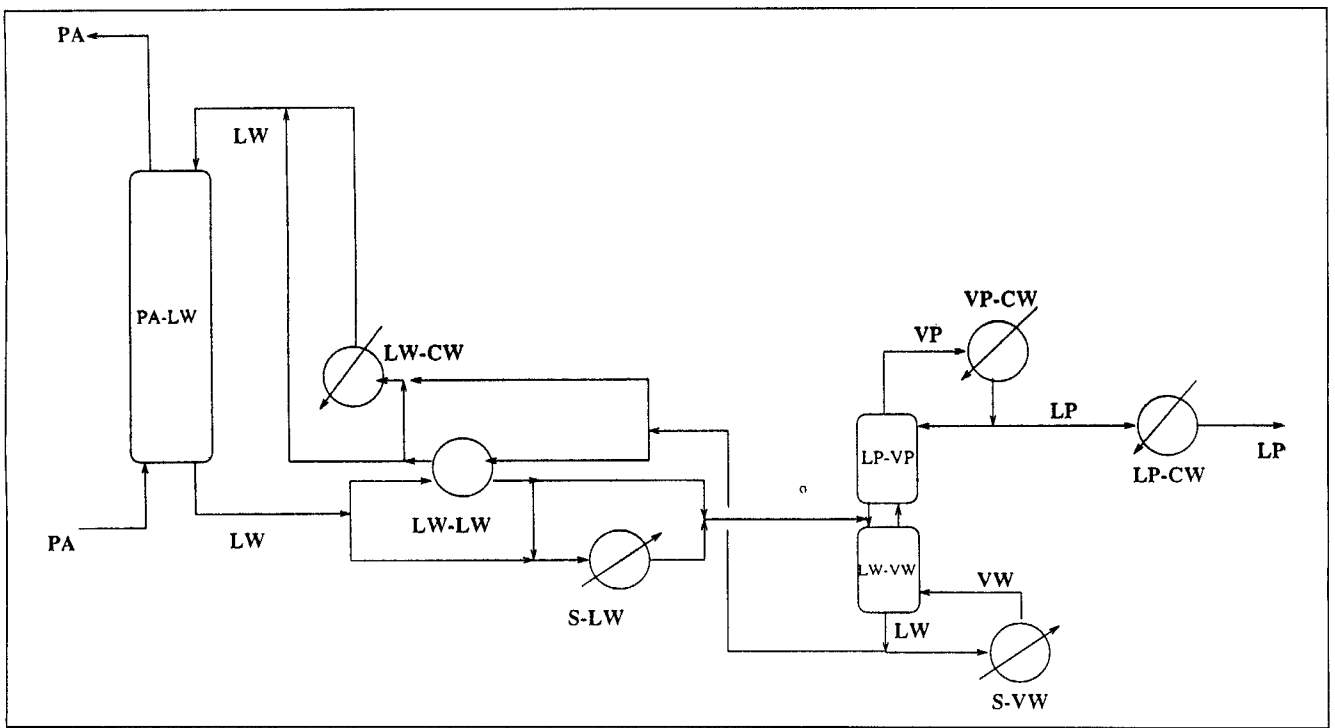


Figure 11. Acetone recovery system: initial structure.

The reaction rates do not depend on temperature, while the liquid is assumed to leave the reactions at bubble point.

A production rate of 10 kmol/h of ethylbenzene is required at a minimum purity of 99.5% from pure benzene. The objective is to explore production schemes based on operating and capital costs.

Since ethylene does not affect the reaction rates and is completely consumed, it is not considered explicitly but only

in operating cost factors, through the final product amounts. Thus, we consider benzene (A) to react to ethylbenzene (B), which further transforms to diethylbenzene (C).

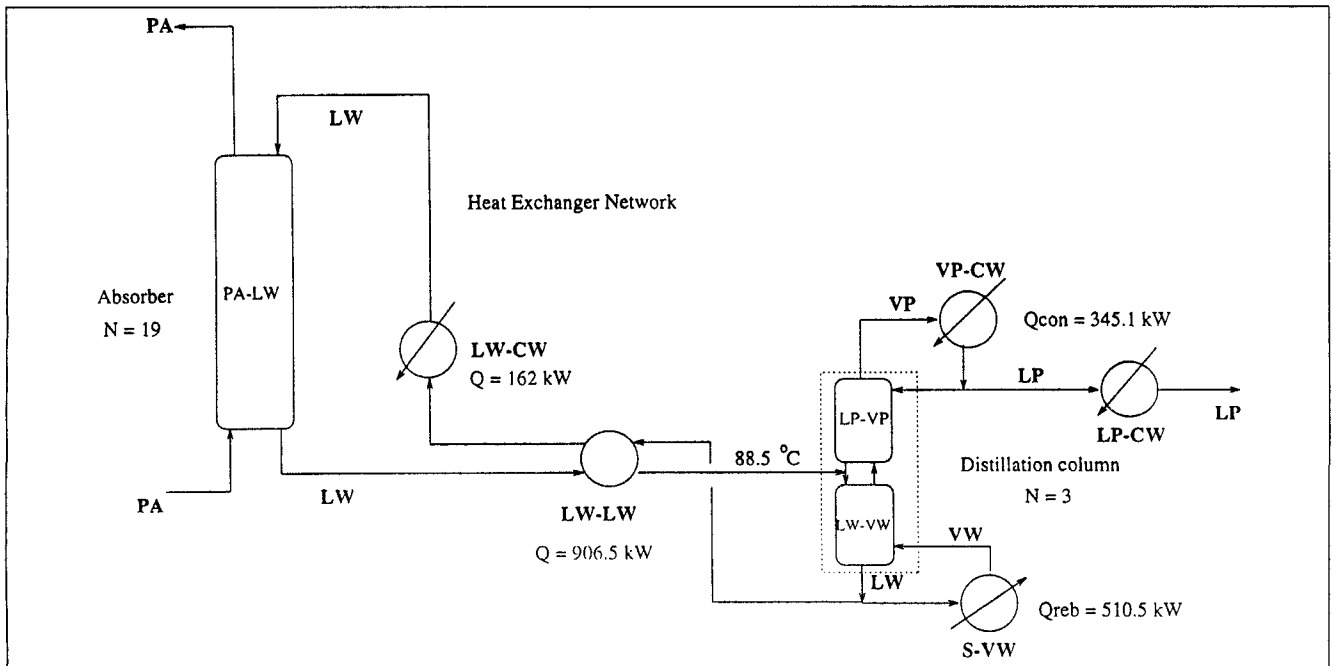


Figure 12. Acetone recovery system: final structure.

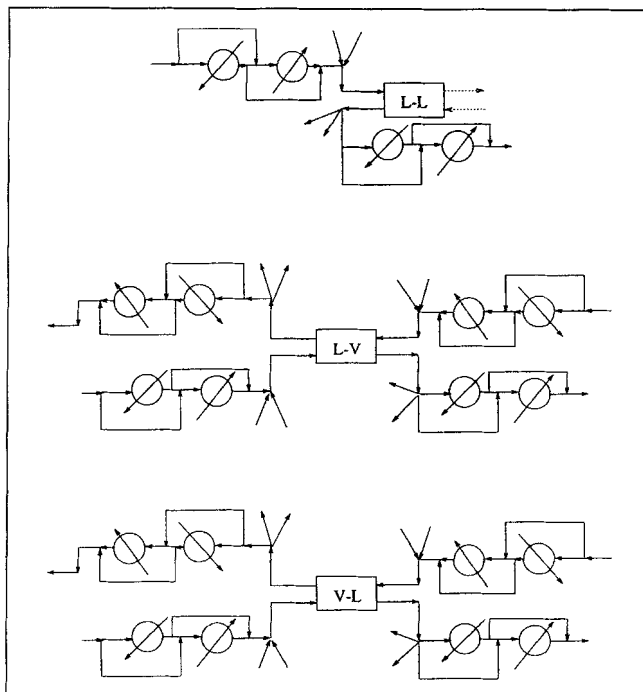


Figure 13. Superstructure modules for benzene alkylation.

The reactions take place in the liquid phase and the desired product (**B**) must be separated. Since all the considered components can be present in both liquid and vapor phases, we consider one mixture stream present in the liquid and the vapor phase as intermediate streams:



and also existing streams $L(A)$, $L(B)$ and outlet stream $L(C)$, which may correspond to multiple instances of $L(ABC)$.

We consider five $L-L$ mass/heat-exchange matches, two $V-L$ matches, where **B** is transferred from vapor to liquid, and two $L-V$ matches, where **B** is transferred to the liquid phase, and all possible utility heat exchangers (heaters and coolers) (Figure 13).

Mixed integer optimization techniques are employed. The existence of each exchange block is denoted by a binary variable. The synthesis model involves 61 binary variables, corresponding to 9 mass/heat- and 52 pure heat-exchange blocks. Note that Kokossis and Floudas (1991) use 36 binary variables for a more detailed representation of a PFR, but without intermediate heating and/or cooling, and corresponding number of equations (mass and energy balances). Operating cost includes: (1) benzene cost, (2) ethylene cost, (3) steam and cooling water cost. Cost data are given in Table 4.

Table 4. Operating Cost Data for Benzene Alkylation

Utility	Cost
Benzene	\$4.92/kmol·yr
Ethylene	\$12.98/kmol·yr
Cooling water	\$24.5/kW·yr
Steam	\$146.8/kW·yr

Minimization of operating cost only led to the process network of Figure 14a. Pure benzene (10 kmol/h) are fed to a battery of reaction blocks (PFR), while the reaction product is first fed to a separation block, where (**A**) is separated and recycled, and then to a purification block, where (**B**) is removed from the top. This configuration features an operating cost of \$851,087/yr.

Simplified capital cost functions are then introduced to the synthesis model. The reactor is sized as PFR, based on its total volume, while the two separation blocks ($V-L$, $L-V$), which may compose more than one mass/heat exchange blocks, in general, are sized as distillation columns, based on feed flow and compositions (Kokossis and Floudas, 1991). $V-L$ matches are treated as part of a column, where (**A**) is separated from (**BC**), while $L-V$ matches are treated as part of a B/C column. Cost functions are given in Table 5.

Optimization of total cost results in the same network structure with different equipment sizes and flows. The new process network (Figure 14b) features a total annualized cost of \$1,348,156/yr (with an operating cost of \$1,032,868/yr).

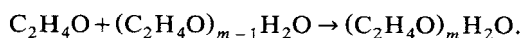
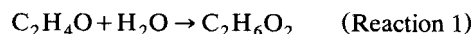
One can note that the separation blocks are not conventional distillation columns (reflux ratio = 0), and the feed enters the "columns" at the top. This may be due to the fact that column operation has not been modeled explicitly (which may be done at a second stage). Limiting the model to more conventional structures (see Figure 15) increases the total process cost (\$1,354,560/yr).

It must be noted that the obtained solution is limited to a maximum of five $L-L$ blocks, forming a PFR and two columns, since we have postulated two sets of $L-V$ and $V-L$ blocks. More postulated blocks might give more realistic or complicated solutions, where each block would correspond to a column tray. However, this would increase the computational complexity of the problem.

Example 3: production of ethylene glycol

The production of ethylene glycol has been revisited recently, since the highly exothermic reactions involved can be exploited in a simultaneous reaction/separation system (reactive distillation). Ciric and Gu (1994) have studied the design of such a reactive distillation column, having postulated as the only alternative a multifeed distillation column, where the reaction takes place in the liquid holdup and employing a tray-by-tray model. Ciric and Miao (1994) have further studied steady-state multiplicities in an ethylene glycol reactive distillation column. Here the synthesis task is studied without adhering to any particular process configuration.

Ethylene glycol ($C_2H_6O_2$ or EG) is produced from ethylene oxide (C_2H_4O or EO) and water (H_2O or W), while heavier glycols are also formed as byproducts:



Here we assume that by-product formation is efficiently represented by the reaction toward diethylene glycol (DG):



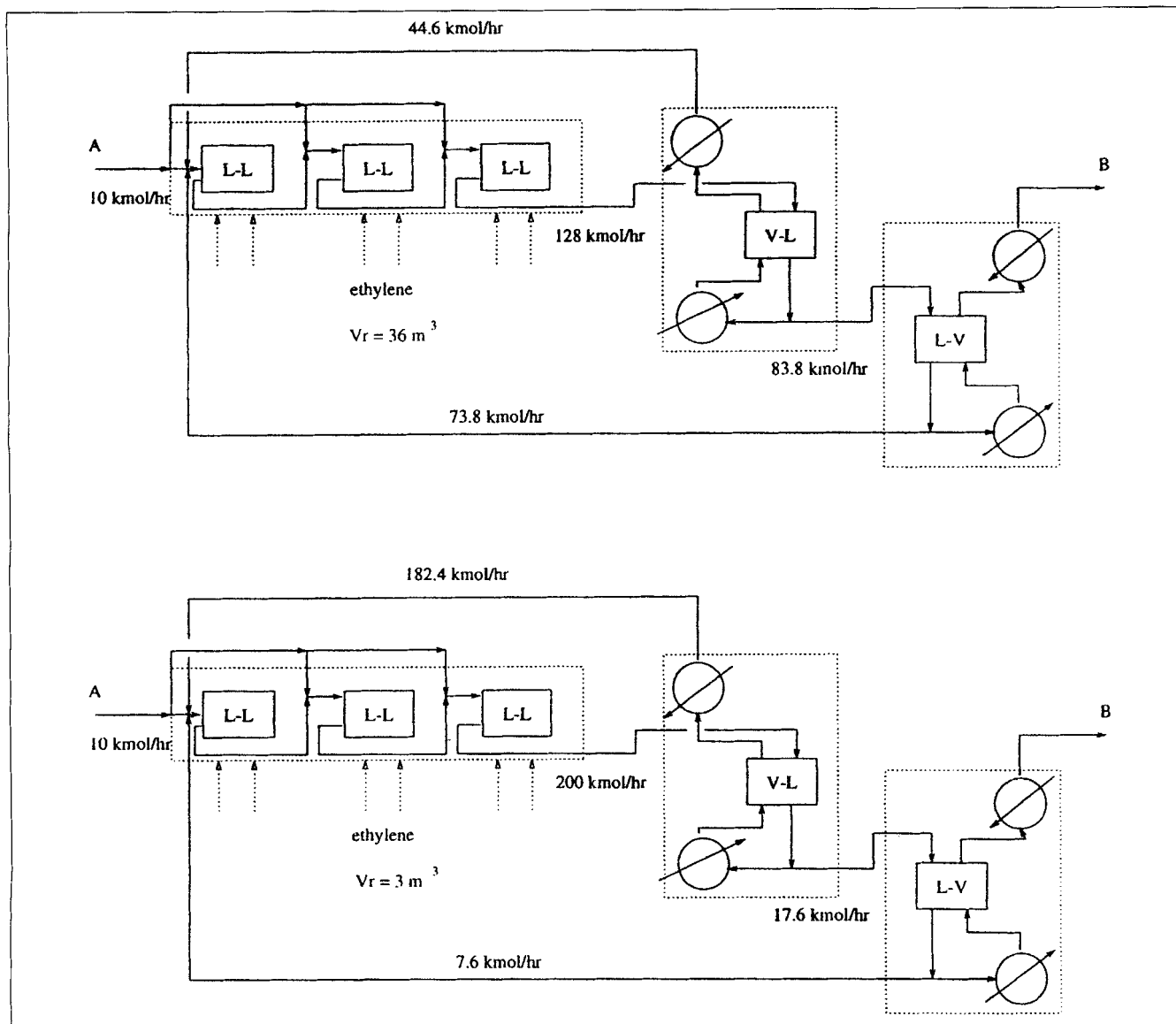


Figure 14. Alkylation of benzene.

(a) Minimum operating cost; (b) minimum TAC.

Both reactions are highly exothermic and assumed to occur in the liquid phase only, while product purification is aided by the large volatility difference of the components of the reaction product mixture. Physical and chemical data are given in Table 6.

A production rate of 25 kmol/h of a stream 95% rich in EG is desired. The synthesis task is studied on the basis of minimum operating cost only. Cost data are given in Table 7.

Since the four components that characterize the synthesis task can all be present in one stream mixture, in the liquid

and the vapor phase, the stream superset involves only *one liquid and one vapor intermediate streams*:

$$L\{EO, W, EG, DG\} \quad \text{and} \quad V\{EO, W, EG, DG\},$$

and two outlet product streams defined by the problem objectives, that is, $L(EG)$ and $L(DG)$, which may be considered as multiples instances of $L\{EO, W, EG, DG\}$.

We consider five mass/heat-exchange matches ($L\{EO, W, EG, DG\}-L\{EO, W, EG, DG\}$), since reactions can take place in the liquid phase only and 15 mass/heat-exchange matches ($V\{EO, W, EG, DG\}-L\{EO, W, EG, DG\}$), since we may have mass transfer due to phase change and high volatility difference and all possible utility heating and cooling heat exchangers (the superstructure modules are similar to the ones in Figure 13). Representing each match with a binary

Table 5. Capital Cost Functions for Benzene Alkylation

Equipment	Annualized Cost
Reactor	$\$12,760.43 + 14,059.8V/\text{yr}$
Column A/BC	$\$41,357.3 + F(432.7 + 418.42x_A - 152.4x_B)/\text{yr}$
Column B/C	$\$54,966.4 + F(748.6x_B - 588.7x_B^2)/\text{yr}$

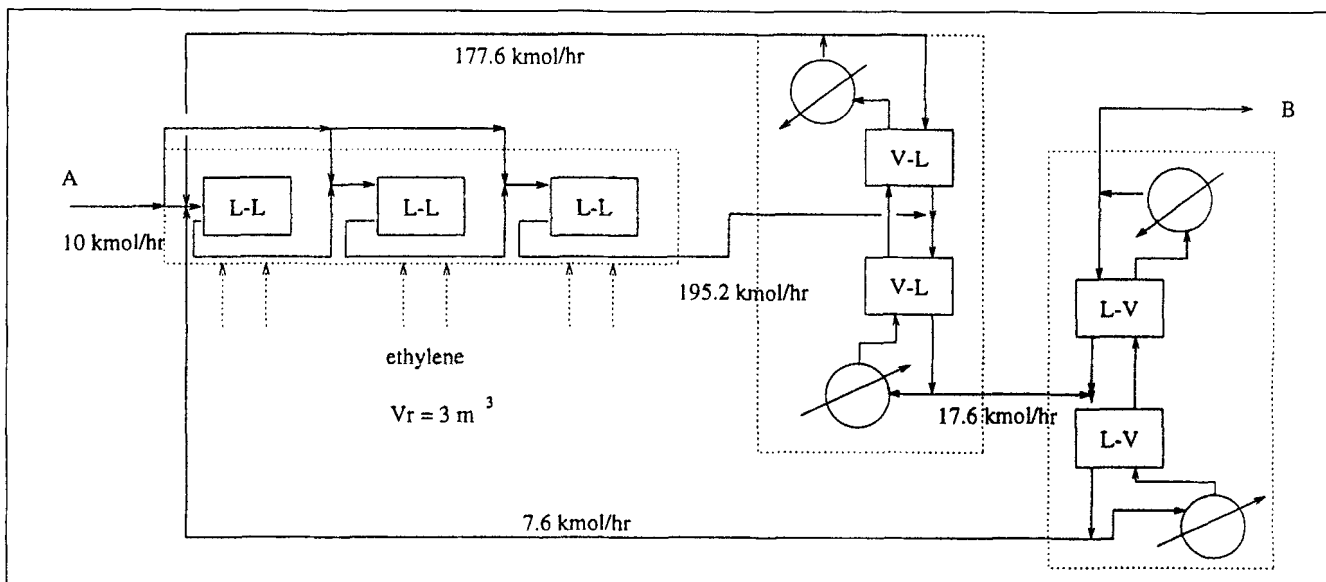


Figure 15. Conventional columns in benzene alkylation.

variable and considering all possible interconnections between blocks, the synthesis problem is formulated as a MINLP, featuring 140 binary variables (20 for mass/heat transfer and 120 for pure heat-transfer blocks). Details of the mass/heat-exchange superstructure model are given in Appendix B; Table 8 depicts a typical equation-variable incidence matrix for the $L-V$ reactive module.

As shown in the section 4 titled "Reactive distillation" (Figures 6 and 7), conventional and nonconventional alternatives are simultaneously encountered in the proposed representation framework. Minimization of operating cost, which includes raw material cost, purification, and utility cost, results in the process structure of Figure 16, featuring a reactive distillation column with two reaction zones and multiple feeds. The operating cost of the column is 1.17×10^6 USD/yr. Temperature and composition profiles suggest that the proposed solution is indeed one of the multiple steady states, which such a reactive distillation column can have (Figures 17 and 18), as reported by Ciric and Miao (1994).

Table 6. Chemical and Physical Data for Ethylene Glycol Example

Reaction Kinetics	
Reaction	
R1	$3.19 \times 10^9 \exp[-9.547/T(K)] x_{EO} x_W$
R2	$6.3 \times 10^9 \exp[-9.547/T(K)] x_{EO} x_{EG}$
Reaction Heats in kJ/mol	
Reaction	
R1	-80.0
R2	-13.1
Vapor Pressures in atm	
EO	$71.9 \exp\{5.72[T(K) - 469]/[T(K) - 35.9]\}$
W	$221.2 \exp\{6.31[T(K) - 647]/[T(K) - 52.9]\}$
EG	$77.0 \exp\{9.94[T(K) - 645]/[T(K) - 71.4]\}$
DG	$47.0 \exp\{10.42[T(K) - 681]/[T(K) - 80.6]\}$

Example 4: heat integration

Considering all possible initial, intermediate, and final streams in a process also enhances heat integration possibilities, allowing for stream mixing. Chang et al. (1994) studied the synthesis of heat-exchanger networks, incorporating in their procedure options for merging and/or splitting streams. Their approach employs decomposition techniques where minimum utility cost, number of units, and optimal structure are successively determined, being limited, however, to streams with constant heat capacities. The proposed representation framework can also be applied in the synthesis of heat-integrated systems with mixed streams and variable heat capacities.

(a) Consider first the heat-exchanger network problem described in Table 9 (Chang et al., 1994). It involves two hot streams to be cooled (H1 and H2) and three cold streams (C1, C2, and C3) to be heated and mixed to give two product-cold streams (C4 and C5). The problem *stream superset* is constructed, including the hot streams (H1 and H2), the initial and final cold streams, (C1, C2, C3, C4, C5), and the mixture of the initial cold streams (C123). Multiple heat-exchange matches are considered for the cold mixture and the hot streams and all the possible interconnections between them (see Figures 19 and 20). The HEN synthesis problem is formulated as a MINLP, involving seven possible exchangers and featuring 2,990 rows, 2,821 continuous variables, and 68 binary variables (including binary/structural variables for interconnections). A minimum temperature approach of $\Delta T_{min} = 11.1^\circ\text{C}$ is required for feasible heat transfer in each ex-

Table 7. Cost Data for Ethylene Glycol Example

EO	\$43.7/kmol
W	\$21.9/kmol
H ₂ O in effluent	\$15 /kmol
Cooling	\$24.5/kW·yr
Heating	\$146.8/kW·yr

Table 8. Modeling Equations and Variables for L-V Reactive Module

Equations	Comp. Mass Balances (4 Comp.)	Mass Exch. Definition (4 Comp.)	Energy Balance	Driving Force (2 Outlets)	Reaction Constant Calc.	Reaction Enthalpy Calc.	Phase Equi. Constant Calc.	Stream Enthalpy Calc.
<i>Lean side</i>								
Stream in								
Flow	X	X	X					
Composition (4 Comp.)	X	X		X				X
Temp.					X	X	X	X
Enthalpy			X					X
Phase								
Eq. const. (4 comp.)				X			X	
Stream out								
Flow	X	X	X					
Composition (4 comp.)	X	X		X				X
Temp.					X	X	X	X
Enthalpy			X					X
Phase								
Eq. const. (4 comp.)				X			X	
<i>Rich Side</i>								
Stream in								
Flow	X	X	X					
Composition (4 comp.)	X	X		X				X
Temp.					X	X	X	X
Enthalpy			X					X
Phase								
Eq. const. (4 comp.)				X			X	
Stream Out								
Flow	X	X	X					
Composition (4 comp.)	X	X		X				X
Temp.					X	X	X	X
Enthalpy			X					X
Phase								
Eq. Const. (4 comp.)				X			X	
Mass exch. (4 comp.)	X	X						
Reaction vol.	X	X	X					
Reaction enthalpy			X			X		
Reaction const.	X	X	X		X			

changer. The proposed network (obtained in 3 GBD iterations and 101 CPU seconds on a SPARC5 workstation computer) is illustrated in Figure 21 and is similar to the solution proposed by Chang et al. (1994).

(b) In order to illustrate the possibility of accounting for variable heat capacities, consider the example problem described in Table 10 (industrial problem). Five hot process streams must be cooled, resulting in three final hot streams, while three cold process streams must be heated, giving two final cold streams. All streams are multicomponent mixtures (13 components) with variable heat capacities (depending on temperature and composition). Composition and heat capacity data are given in Tables 11 and 12. Streams can be mixed as illustrated in Table 10. Three hot utilities are available (three-level steam), as well as cooling water (cost data given in Table 13). All possible streams and heat-exchange matches

are considered (Table 14), resulting in a superstructure with 29 possible heat exchangers. The MINLP model features 5,018 rows, 857 continuous variables, and 423 binary variables. The optimal heat-exchanger network (obtained in 60.5 CPU seconds on a SPARC10 workstation computer) is illustrated in Figure 22. It involves stream mixing at several temperature levels and corresponds to a total annualized cost of \$122,080/yr.

Discussion

The application of the proposed process synthesis modeling and representation framework, and the synthesis procedure of Figure 8 to the example problems revealed a number of issues that deserve some further discussion.

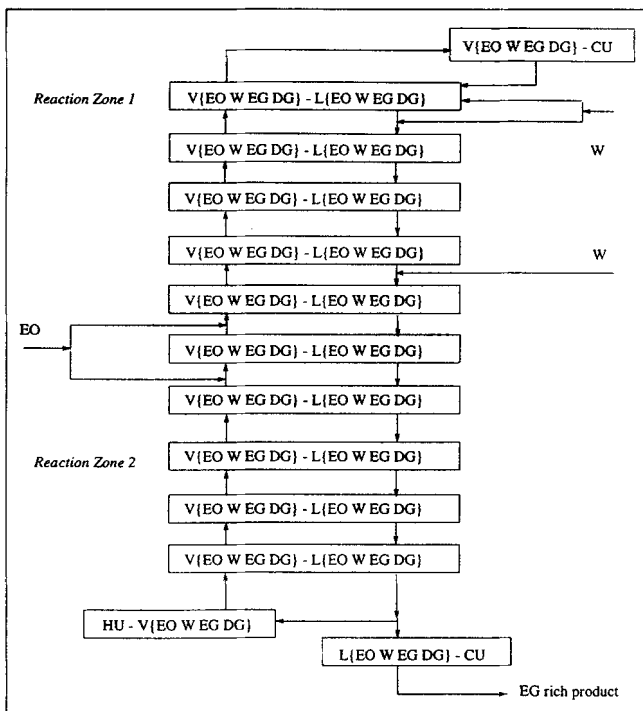


Figure 16. Reactive distillation for ethylene glycol production.

For the case of conventional process flowsheets, as for example the acetone recovery process in Example 1, the resulting model by the suggested representation, despite being much more general, compares favorably to the model generated by a unit-based superstructure synthesis representation; its size (127 0-1 variables, 544 continuous variables, and 848

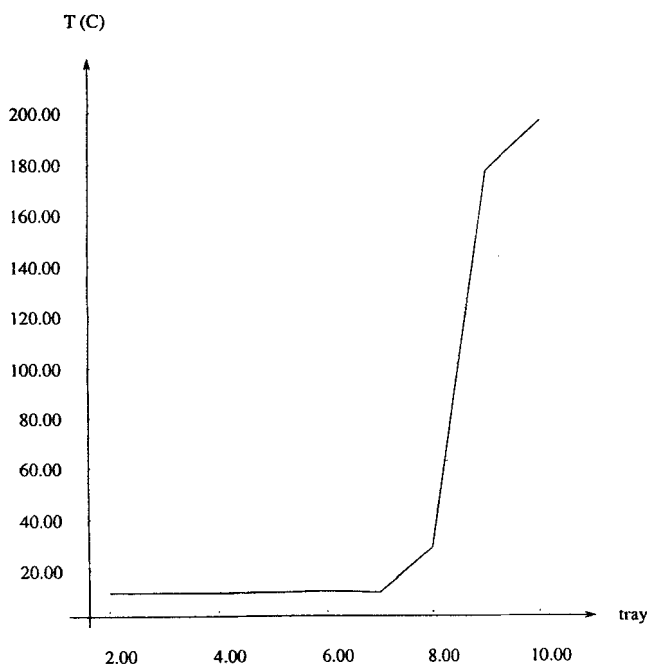


Figure 17. Temperature profile in reactive distillation column.

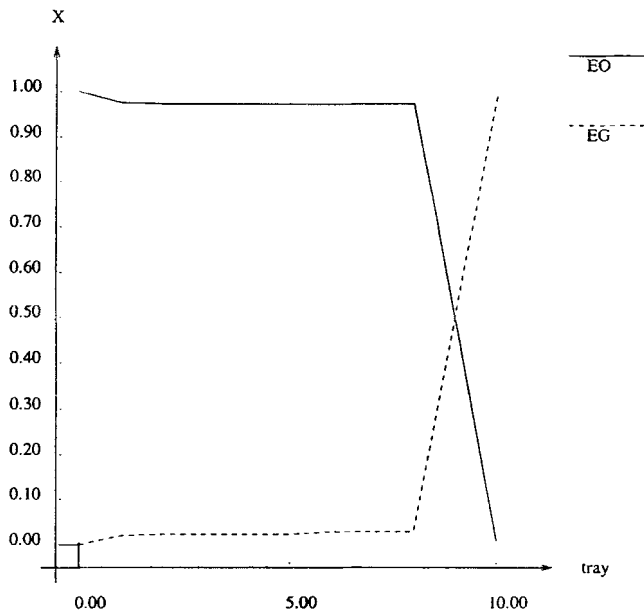


Figure 18. Composition profile in reactive distillation column.

rows) is rather moderate and numerical solutions can be comfortably obtained with existing standard mixed integer optimization techniques. Similar conclusions regarding computational efficiency can also be drawn from the heat integration examples (Example 4), where numerical solutions were obtained in reasonable CPU times, despite the fact that both problem instances (the first case involving mixing and the second involving variable heat capacities of multicomponent mixtures in 13 components) cannot readily be addressed by conventional HEN-superstructure techniques.

For the case of potentially nonconventional process flowsheets, as in Example 2 and 3, a comparison of the model size resulting from the proposed framework to model sizes obtained by unit-based representations, is not as straightforward. In the ethylbenzene process (Example 2), our model allows for the possibility of hybrid units (simplified reactive distillation column), and thus is obviously of larger size (in terms of number of variables and rows, reflecting kinetic constant calculations and heat enthalpies at different conditions). However, at the limit, when "hybrid" options are not considered, and as discussed in the fourth section, the resulting model from our representation is in fact of identical size to unit-based representation (Kokossis and Floudas, 1991; Bagajewicz and Manousiouthakis, 1992).

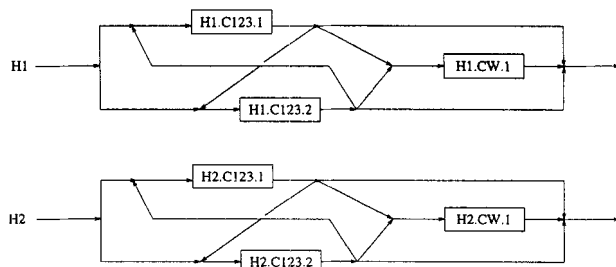


Figure 19. Hot stream superstructure—I.

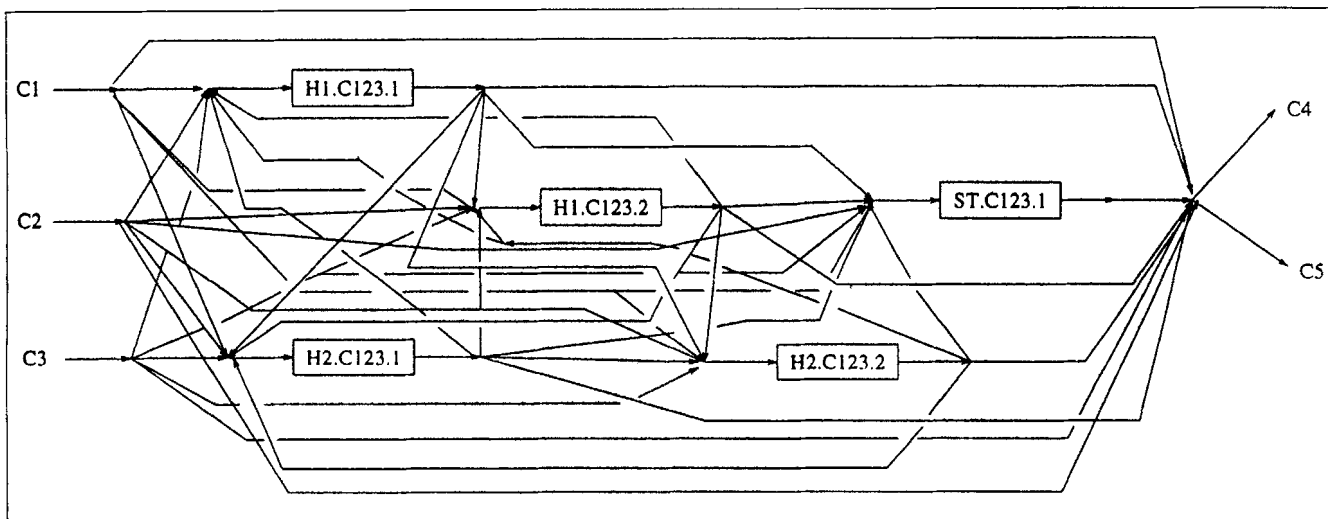


Figure 20. Cold stream superstructure—I.

The advantage of employing a multipurpose representation that is not based on unit postulations, is clearly illustrated in Example 3, where a fair comparison (in terms of model size) has to be done between our model and a postulated unit superstructure of alternatives involving (1) a reactor followed

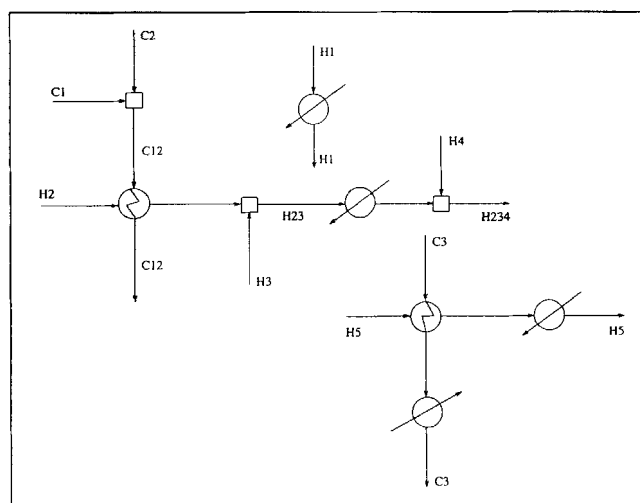


Figure 22. Heat-exchanger network—II.

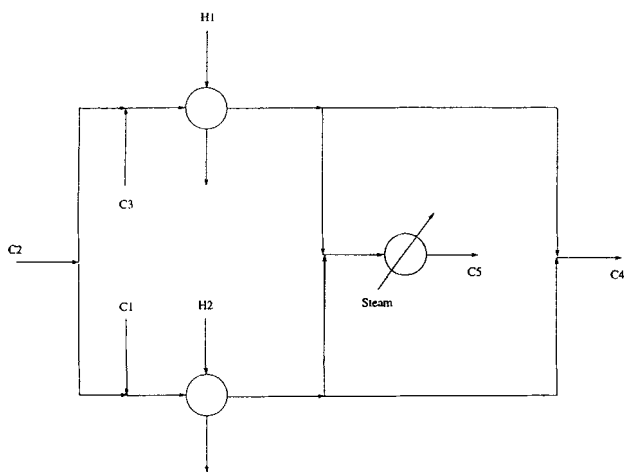


Figure 21. Heat-exchanger network—I.

Table 9. First Example in Heat Integration

Stream	Heat Capacity Flow Rate kW/°C	Inlet Temp. °C	Outlet Temp. °C
H1	16.6	248.9	121.1
H2	13.3	204.4	65.6
C1	11.4	37.8	
C2	12.9	65.6	
C3	13.0	93.3	
C4	24.4		204.4
C5	12.9		182.2
Steam	∞	300	300
Water	∞	20	30

Table 10. Stream Data for Second Example in Heat Integration

Stream	Stream Type	Flow kmol/h	Inlet Temp. °C	Outlet Temp. °C
H1	Initial	84.9	48.5	40
H2	Initial	3,197.2	160.0	—
H3	Initial	30.5	41.9	—
H4	Initial	131.2	42.0	—
H23	Mix. of H2, H3	3,227.8	—	—
H234	Mixt. of H2, H3, H4	3,359.0	—	45
H5	Initial	350.6	123.0	45.0
C1	Initial	122.3	25.0	—
C2	Initial	2,412.0	48.5	—
C12	Mix. of C1, C2	2,534.4	—	105.5
C3	Initial	1,326.5	62.0	76.6
HS1	High-Pres. Steam	∞	240.0	240.0
HS2	Medium-Pres. Steam	∞	182.0	182.0
HS3	Low-Pres. steam	∞	140.0	140.0
CW	Cooling Water	∞	20.0	25.0

Table 11. Stream Compositions for Second Example in Heat Integration

	Molecular Fraction												
	C1	C2	C3	C4	C5	C6	C7	C8	C9	C10	C11	C12	C13
H1	0.117	0.059	0.038	0.023	0.048	0.036	0.414	0.000	0.000	0.000	0.261	0.000	0.000
H2	0.088	0.044	0.028	0.017	0.000	0.027	0.319	0.070	0.000	0.000	0.295	0.106	0.001
H3	0.005	0.003	0.003	0.001	0.557	0.005	0.397	0.018	0.001	0.000	0.005	0.003	0.000
H4	0.075	0.038	0.040	0.015	0.794	0.022	0.010	0.000	0.000	0.000	0.004	0.000	0.000
H5	0.000	0.000	0.000	0.000	0.000	0.000	0.000	0.000	0.001	0.000	0.175	0.823	0.001
C1	0.000	0.000	0.000	0.002	0.996	0.001	0.000	0.000	0.001	0.000	0.175	0.823	0.001
C2	0.117	0.059	0.038	0.023	0.048	0.036	0.414	0.000	0.000	0.000	0.261	0.000	0.000
C3	0.000	0.000	0.000	0.000	0.000	0.000	0.000	0.001	0.001	0.000	0.913	0.085	0.000

by a distillation column with all possible types of heating and cooling options, and (2) a reactive distillation column, with the detailed models for each respective case. Considering that the representation proposed in this work essentially embodies both alternatives in a unified way, the size of the resulting model cannot exceed the corresponding model in the unit-based case. Actually, due to the "multipurpose" character of the mass/heat and heat-transfer modules, in the case of potentially nonconventional process structures, a much more compact model will in general result. It is also interesting to note that as soon as a reactive distillation column emerges as a promising design alternative after the optimization in the first step of the synthesis procedure, the generated model in the second step (optimization of total annualized cost) for the reactive distillation column would be in fact identical in size to the one proposed by Ciric and Gu (1994). It should also be noted that the explicit heat inclusion of heat integration schemes (heat exchange modules) adopted in this representation are mostly attributable to large model sizes.

The incorporation of detailed models and capital cost aspects have been proposed here in a second optimization step, after conventional and nonconventional structural synthesis alternatives have been investigated (see Figure 8). Example 2

shows the application of such a hierarchical synthesis procedure. First, operating cost optimization leads to an initial process structure with the proposition of the required units, whereas detailed cost models are employed in a second optimization step (following the general guidelines of Douglas's hierarchical approach). Obviously, such a synthesis procedure may not necessarily result in a global optimal solution.

The detailed representation of conventional and/or nonconventional process schemes through sets of mass/heat and pure heat-transfer modules depends largely on the initial number of postulated mass/heat exchange matches. In Example 2, a PFR is represented by at most five ideally mixed mass/heat-transfer modules, which might not correspond to realistic mixing patterns. As the number of initially postulated mass/heat-exchange matches increases, the quality of representation in the proposed framework improves, albeit the synthesis model becomes more complex. Determining the "optimal" number of postulated mass/heat-transfer modules that is required to efficiently represent process synthesis alternatives is clearly a challenging and yet open question.

Nevertheless, the complexity of the resulting synthesis problems is mostly attributed to conventional nonlinear models commonly employed in any physicochemical system. In this

Table 12. Physical Properties for Second Example in Heat Integration

$C_p = AT(^{\circ}C) + B(\text{kJ/kmol})$													
	A	C1	C2	C3	C4	C5	C6	C7	C8	C9	C10	C11	C12
H1	-0.002	-0.003	0.003	0.037	0.083	0.107	0.029	-0.505	-0.733	-1.148	-8.268	0.495	-4.339
H2	0.001	-0.001	0.008	0.056	0.091	0.120	0.028	0.093	0.111	0.104	-0.321	1.597	-0.189
H3	-0.002	-0.003	0.002	0.035	0.082	0.104	0.031	-0.570	-0.846	-1.337	-10.965	0.430	-5.961
H4	-0.002	-0.003	0.003	0.036	0.084	0.008	0.032	0.000	0.000	0.000	-8.716	0.000	0.000
H5	0.000	0.000	0.000	0.000	0.000	0.000	0.000	0.000	0.000	0.000	0.143	0.643	0.568
H23	0.001	-0.001	0.008	0.056	0.091	0.120	0.028	0.093	0.111	0.104	-0.321	1.597	-0.189
H234	0.001	-0.001	0.008	0.056	0.091	0.120	0.028	0.093	0.111	0.104	-0.321	1.597	-0.189
C1	0.000	0.000	0.000	0.025	0.060	0.072	0.000	0.000	0.000	0.000	0.000	0.000	0.000
C2	-0.002	-0.003	0.003	0.037	0.083	0.107	0.029	-0.505	-0.733	-1.148	-8.268	0.495	-4.339
C12	-0.002	-0.003	0.003	0.037	0.083	0.107	0.029	-0.505	-0.733	-1.148	-8.268	0.495	-4.339
C3	0.000	0.000	0.000	0.000	0.000	0.000	0.000	0.288	0.285	0.144	0.098	0.552	0.556
B													
H1	29.62	21.32	29.75	35.57	43.22	52.93	39.04	176.61	211.37	260.65	683.53	534.95	632.92
H2	29.23	21.11	29.19	33.86	42.53	51.85	39.11	125.51	140.09	156.78	99.21	-51.15	290.63
H3	29.56	21.25	29.70	35.56	42.95	52.57	38.63	170.63	205.24	253.34	729.33	56.45	692.15
H4	29.54	21.23	29.67	35.47	42.82	52.38	38.55	0.00	0.00	0.00	637.81	0.00	0.00
H5	0.00	0.00	0.00	0.00	0.00	0.00	0.00	0.00	0.00	0.00	60.75	616.15	208.68
H23	29.23	21.11	29.12	33.86	42.53	51.85	39.11	125.51	140.09	156.78	99.21	-51.15	290.63
H234	29.23	21.11	29.19	33.86	42.53	51.85	39.11	125.51	140.09	156.78	99.21	-51.15	290.63
C1	0.00	0.00	0.00	36.56	45.28	55.85	0.00	0.00	0.00	0.00	0.00	0.00	0.00
C2	29.62	21.32	29.75	35.57	43.22	52.93	39.04	176.61	211.37	260.65	683.53	53.49	632.92
C3	0.00	0.00	0.00	0.00	0.00	0.00	0.00	147.65	163.56	182.75	65.10	70.08	209.797
C12	29.62	21.32	29.75	35.57	43.22	52.93	39.04	176.61	211.37	260.65	683.53	53.49	632.92

Table 13. Cost Data for Second Example in Heat Integration

HS1	\$84 /kW·yr
HS2	\$65.5/kW·yr
HS3	\$61.5/kW·yr
CW	\$7.26/kW·yr

respect, the numerical difficulties that potentially arise here are not due to the proposed representation, but rather reflect limitations of current nonlinear-based optimization techniques and codes, and in fact also arise in conventional optimization and even simulation synthesis methods. Combinatorial explosion still remains a problem; yet, in most physicochemical systems total superstructure connectivity is not a sensible option. Here, prescreening based on sound engineering knowledge and physical laws is important; such a prescreening process can in principle be encoded in the form of logic constraints that can then be readily incorporated in the mathematical model. The development of logic-based techniques together with tailor-made mixed integer optimization methods, as in the work by Raman and Grossmann (1993), will help alleviate some of these difficulties.

The representation framework, proposed in this article provides a platform for a synthesis procedure, hierarchical or simultaneous, which is not trapped in conventional synthesis schemes, but free to identify "hybrid" units and structures. Clearly, work is still required to support the initial promising results reported in this article to other synthesis problems, where even physicochemical phenomena may not be conventional.

Conclusions

A representative framework for process synthesis alternatives, based on broadened concepts of mass and heat transfer in process operations, has been proposed in this article. A mass/heat-exchange superstructure module has been introduced as the building block of entire process flowsheets, involving reactors, separations, and so forth. The representation scheme has been coupled with synthesis guidelines toward a generalized process synthesis framework, where synthesis alternatives are explored without prepostulating unit networks. A variety of examples are presented to illustrate the applicability of the proposed framework to different synthesis problems. Limitations of current synthesis methods are overcome, as in HEN synthesis problems, or in more general problems, where nonconventional synthesis schemes are identified.

Table 14. Stream Matches for Second Example in Heat Integration

Matches Hot Stream	Cold Stream
H1	C1,C12,C3,CW
H2	C1,C12,C3,CW
H23	C1,C12,C3,CW
H234	C1,C12,C3,CW
H5	C1,C12,C3,CW
HS1	C1,C12,C3
HS2	C1,C12,C3
HS3	C1,C12,C3

Acknowledgments

Financial support from the European Communities, under contract N.JOU2-CT93-0369, is greatly acknowledged.

Notation

- c = molar fraction
- f^I = flow to exchanger from initial splitter
- f^{in} = inlet flow to exchanger
- f^{out} = outlet flow from exchanger
- $f_{V-L}^{\beta,L-L}$ = bypass flow from $L-L$ exchanger to $V-L$ exchanger
- Cal** = cooler after lean side
- Car** = cooler after rich side
- Cbl** = cooler before lean side
- Cbr** = cooler before rich side
- DH^{r1}, DH^{r2} = reaction enthalpies
- h = molar enthalpy
- Hal** = heater after lean side
- Har** = heater after rich side
- Hbl** = heater before lean side
- Hbr** = heater before rich side
- k = phase equilibrium constant
- k^{r1}, k^{r2} = kinetic constants
- $M_{V-L}^{reac,EG}$ = reacted mass
- $M_{V-L}^{trans,EG}$ = mass transferred due to phase change
- VL** = exchanger liquid volume (holdup)

Literature Cited

Achenie, L. K. E., and L. T. Biegler, "A Superstructure Based Approach to Chemical Reactor Network Synthesis," *Comput. Chem. Eng.*, **14**, 23 (1990).

Aggarwal, A., and C. A. Floudas, "Synthesis of Heat integrated Non-sharp Distillation Sequences," *Comput. Chem. Eng.*, **16**, 89 (1992).

Bagajewicz, M. J., and V. Manousiouthakis, "Mass/Exchange Network Representation of Distillation Networks," *AIChE J.*, **38**, 1769 (1992).

Balakrishna, S., and L. T. Biegler, "A Unified Approach for the Simultaneous Synthesis of Reaction, Energy and Separation Systems," *Ind. Eng. Chem. Res.*, **32**, 1372 (1993).

Brooke, A., D. Kendrick, and A. Meeraus, *GAMS: A User Guide*, Scientific Press, Redwood City, CA (1988).

Chang, C. T., K. K. Chu, and J. R. Hwang, "Application of the Generalized Stream Structure in HEN Synthesis," *Comput. Chem. Eng.*, **18**, 345 (1994).

Chitra, S. P., and R. Govind, "Synthesis of Optimal Serial Reactor Structures for Homogeneous Reactions: I and II," *AIChE J.*, **31**, 177 (1985).

Circ, A. R., and C. A. Floudas, "Heat Exchanger Network Synthesis without Decomposition," *Comput. Chem. Eng.*, **15**, 385 (1991).

Circ, A. R., and D. Gu, "Synthesis of Nonequilibrium Reactive Distillation Processes by MINLP Optimization," *AIChE J.*, **40**, 1479 (1994).

Circ, A. R., and P. Miao, "Steady State Multiplicities in an Ethylene Glycol Reactive Distillation Column," *Ind. Eng. Chem. Res.*, **33**, 2738 (1994).

Circ, A. R., and T. Jia, "Economic Sensitivity Analysis of Waste Treatment Cost in Source Reduction Projects: Continuous Optimization Problems," *AIChE Meeting*, Los Angeles (1991).

Douglas, J. M., *Chemical Design of Chemical Processes*, McGraw Hill, New York, (1988).

Duran, M. A., and I. E. Grossmann, "A Mixed Integer Nonlinear Programming Algorithm for Process Synthesis," *AIChE J.*, **32**, 592 (1986).

El-Halwagi, M. M., and V. Manousiouthakis, "Synthesis of Mass Exchange Networks," *AIChE J.*, **35**, 1233 (1989).

Floudas, C. A., Separation Synthesis of Multicomponent Feed Streams into Multicomponent Product Streams," *AIChE J.*, **33**, 540 (1987).

Floudas, C. A., and G. E. Paules, "A Mixed Integer Nonlinear Programming Formulation for the Synthesis of Heat Integrated Distillation Sequences," *Comput. Chem. Eng.*, **12**, 531 (1988).

Friedler, F., K. Tarjan, Y. W. Huang, and L. T. Fan, "Graph Theoretic Approach to Process Synthesis: Polynomial Algorithm for Maximal Structure Generation," *Comput. Chem. Eng.*, **17**, 929 (1993).

Grossmann, I. E., and M. M. Daichendt, "New Trends in Optimization-based Approaches in Process Synthesis," *Proc. PSE*, p. 95. (1994).

Hendry, J. E., D. F. Rudd, and J. D. Seader, "Synthesis in the Design of Chemical Processes," *AIChE J.*, **19**, 1 (1973).

Knight, J. R., and M. F. Doherty, "Optimal Design and Synthesis of Homogeneous Azeotropic Distillation Sequences," *Ind. Eng. Chem. Res.*, **28**, 564 (1989).

Kocis, G. R., and I. E. Grossmann, "Relaxation Strategy for the Structural Optimization of Process Flowsheets," *Ind. Eng. Chem. Res.*, **26**, 1869 (1987).

Kocis, G. R., and I. E. Grossmann, "A Modelling and Decomposition Strategy for the MINLP Optimization of Process Flowsheets," *Comput. Chem. Eng.*, **13**, 797 (1989).

Kokossis, A. C., and C. A. Floudas, "Optimization of Complex Reactor Networks: I. Isothermal Operation," *Chem. Eng. Sci.*, **45**, 595 (1990).

Kokossis, A. C., and C. A. Floudas, "Synthesis of Isothermal Reactor-Separator-Recycle Systems," *Chem. Eng. Sci.*, **46**, 1361 (1991).

Kokossis, A. C., and C. A. Floudas, "Optimization of Complex Reactor Networks: II. Nonisothermal Operation," *Chem. Eng. Sci.*, **49**, 1037 (1994).

Nishida, N., G. Stephanopoulos, and A. W. Westerberg, "A Review of Process Synthesis," *AIChE J.*, **27**, 321 (1981).

Papdlexandri, K. P., and E. N. Pistikopoulos, "Synthesis and Retrofit Design of Operable Heat Exchanger Networks: I and II," *Ind. Eng. Chem. Res.*, **33**, 1718. (1994).

Papdlexandri, K. P., E. N. Pistikopoulos, and C. A. Floudas, "Mass Exchange Networks for Waste Minimization: A Simultaneous Approach," *Trans. Ind. Chem. Eng., Part A*, **72**, 279 (1994).

Quesada, I., and I. E. Grossmann, "Global Optimization Algorithm of Process Networks with Multicomponent Flows," *AIChE Meeting*, St. Louis (1993).

Raman, R., and I. E. Grossmann, "Symbolic Integration of Logic in Mixed Integer Linear Programming Techniques for Process Synthesis," *Comput. Chem. Eng.*, **17**, 909 (1993).

Rigg, T. J., and R. E. Swaney, "Synthesis of General Equilibrium-based Separation Processes Using a Network Flow Model," *Proc. PSE*, p. 55 (1994).

Sargent, R. W. H., "A Functional Approach to Process Synthesis and its application to Distillation Systems," *Comput. Chem. Eng.*, (1994), submitted.

Sargent, R. W. H., and K. Gaminibandara, *Optimization in Action*, Vol. 12, Chap. Introduction: Approaches to Chemical Process Synthesis," Academic Press, London, p. 531 (1976).

Siirola, J. J., "An Industrial Perspective on Process Synthesis," *AIChE Symp. Ser.*, **91**, 222 (1995).

Wehe, R. P., and A. W. Westerberg, "An Algorithmic Procedure for the Synthesis of Distillation Sequences with Bypass," *Comput. Chem. Eng.*, **11**, 619 (1987).

Yee, T. F., and I. E. Grossmann, "Simultaneous Optimization Models for Heat Integration: II. Heat Exchanger Network Synthesis," *Comput. Chem. Eng.*, **14**, 1165 (1990).

Appendix A: Mass/Heat-Exchange Superstructure Model for Acetone Recovery Example

The mass/heat exchange superstructure in the acetone recovery example involves 4 mass/heat transfer blocks and 12 pure heat exchangers (Figure 9). The synthesis model involves:

Mass balances for total stream flows:

- At initial stream splitters, for example, at the initial splitter of PA:

$$F_{PA}^{in} = f_{PA,PA-LP}^{Rin} + f_{PA,PA-LW}^{Rin}$$

where F_{PA}^{in} is the total flow of air mixture, and $f_{PA,PA-LP}^{Rin}$, $f_{PA,PA-LW}^{Rin}$ are the flows toward its potential exchangers (Figure 9).

- at stream splitters at the outlet of each exchange block (mass/heat or pure heat), for example, at the lean side splitter after PA-LW:

$$\begin{aligned} f_{PA-LW}^{L,out} = & f_{LW-VW}^{LBR,PA-LW} + f_{LP-VP}^{LBR,PA-LW} + f_{PA-LP}^{LBL,PA-LW} \\ & + f_{PA-LW}^{LBH,PA-LW} + f_{LP-LP}^{LBH,PA-LW} + f_{LP-LW}^{LBH,PA-LW} + f_{LP-CW}^{LBH,PA-LW} \\ & + f_{LW-LP}^{LBH,PA-LW} + f_{LW-LW}^{LBH,PA-LW} + f_{LW-CW}^{LBH,PA-LW} + f_{LP-LP}^{LBC,PA-LW} \\ & + f_{VP-LP}^{LBC,PA-LW} + f_{LW-LP}^{LBC,PA-LW} + f_{LP-LW}^{LBC,PA-LW} + f_{VP-LW}^{LBC,PA-LW} \\ & + f_{LW-LW}^{LBC,PA-LW} + f_{s-LW}^{LBC,PA-LW} + f_{LP}^{LO,PA-LW} + f_{LW}^{LO,PA-LW}, \end{aligned}$$

where $f_{PA-LW}^{L,out}$ is the flow out of the lean side of exchanger (PA-LW), $f_{LW-VW}^{LBR,PA-LW}$ is the bypass flow from the lean side of (PA-LW) to the rich side of (LW-VW), and so on. The flows just given are possible according to phase-mixing assumptions. However, some of them, for example, $f_{LP-LP}^{LBH,PA-LW}$, which seem improbable, are eliminated by optimization.

- At mixers prior to heat exchanger sides (mass/heat or pure heat), for example, at the lean side mixer prior to PA-LW:

$$\begin{aligned} f_{PA-LW}^{L,in} = & f_{PA-LW}^{LBL,PA-LP} + f_{PA-LW}^{RBL,LW-VW} + f_{PA-LW}^{RBL,LP-VW} \\ & + f_{PA-LW}^{HBL,LP-LP} + f_{PA-LW}^{HBL,LP-LW} + f_{PA-LW}^{HBL,LP-CW} + f_{PA-LW}^{HBL,LW-LP} \\ & + f_{PA-LW}^{HBL,LW-LW} + f_{PA-LW}^{HBL,LW-CW} + f_{PA-LW}^{CBL,LP-LP} + f_{PA-LW}^{CBL,VP-LP} \\ & + f_{PA-LW}^{CBL,LW-LP} + f_{PA-LW}^{CBL,S-LP} + f_{PA-LW}^{CBL,LP-LW} + f_{PA-LW}^{CBL,VP-LW} \\ & + f_{PA-LW}^{CBL,LW-LW} + f_{PA-LW}^{CBL,S-LW} + f_{W,PA-LW}^{L,in}, \end{aligned}$$

where $f_{PA-LW}^{L,in}$ is the flow into the lean side of exchanger (PA-LW), and the rest flows are defined as earlier.

- at final mixers, for example, at the final mixer of acetone-rich liquid product:

$$\begin{aligned} F_{LP}^{out} = & f_{LP,PA-LW}^{LO} + f_{LP,PA-LP}^{LO} + f_{LP,LP-VP}^{RO} + f_{LP,LW-VW}^{RO} \\ & + f_{LP,LP-LP}^{HO} + f_{LP,LP-LW}^{HO} + f_{LP,LP-CW}^{HO} + f_{LP,LW-LP}^{HO} \\ & + f_{LP,LW-LW}^{HO} + f_{LP,LW-CW}^{HO} + f_{LP,LP-LP}^{CO} + f_{LP,VP-LP}^{CO} \\ & + f_{LP,LW-LP}^{CO} + f_{LP,S-LP}^{CO} + f_{LP,LP-LW}^{CO} + f_{LP,VP-LW}^{CO} \\ & + f_{LP,LW-LW}^{CO} + f_{LP,S-LW}^{CO}, \end{aligned}$$

where F_{LP}^{out} is the desired product flow, $f_{LP,PA-LW}$ the flow out from the lean side of PA-LW toward the final mixers of LP, and so forth.

Component mass balances, similar to total flow mass balances:

- At mixers prior to each exchanger side, to determine inlet compositions to the corresponding exchanger side.
- At final mixers of streams, to determine outlet compositions.

• Mass balances for each component at each mass/heat exchanger block, for example, for acetone at PA-LW

$$f_{PA-LW}^{Lin} x_{PA-LW}^{Lin,acet} + f_{PA-LW}^{Rin} x_{PA-LW}^{Rin,acet} - f_{PA-LW}^{Rout} x_{PA-LW}^{Rout,acet} - f_{PA-LW}^{Lout} x_{PA-LW}^{Lout,acet} + \mathfrak{F}(\text{reactions}) = 0,$$

where x 's are compositions, corresponding to flows, and $\mathfrak{F}(\text{reactions})$ accounts for possible generation or consumption of acetone, if any reactions are known to take place in a (PA-LW) system.

Summation of molar fractions (equal to 1) at each mass/heat exchanger outlet.

Enthalpy balances at the mixers of the superstructure, to determine the mixer outlet temperature.

Enthalpy balances at each mass/heat-exchange block, where reaction enthalpy and/or phase change enthalpy are taken into consideration.

Energy balances at each heat-exchange block, accounting for phase-change enthalpy.

Phase-defining constraints at the superstructure mixers and each exchanger outlet, for example, at the outlet of the rich side of (LW-VW):

$$x_{LW-VW}^{Lout,acet} k_{LW-VW}^{Lout,acet} + x_{LW-VW}^{Lout,water} k_{LW-VW}^{Lout,water} \leq 1,$$

where k 's define phase equilibrium constants (note that air may not be possible in this mixture, at moderate conditions).

Driving-force constraints for mass transfer of the component of interest (acetone) at the inlet and outlet of mass/heat exchangers, for example, at the lean outlet of (PA-LW):

$$x_{PA-LW}^{Lout,acet} - k_{PA-LW}^{Lacet} x_{PA-LW}^{Rin,acet} \leq 0,$$

where k_{PA-LW}^{Lacet} is the mass-transfer constant for acetone between PA and LW. Or, at the lean outlet of (LP-VP):

$$x_{LP-VP}^{Lout,acet} - k_{LP-VP}^{Lacet} x_{LP-VP}^{Rin,acet} \leq 0,$$

where k_{LP-VP}^{Lacet} is the mass-transfer constant for acetone between LP and VP (in this case, the phase equilibrium constant).

Temperature driving-force constraints at heat exchangers

The existence of each mass/heat and pure heat-transfer block is denoted by a binary variable and defined by mixed-integer constraints of the type:

$$M_{PA-LW}^{acet,exchange} - y_{PA-LW} \mathbf{U} \leq 0,$$

or equivalently,

$$f_{PA-LW}^{Lout} x_{PA-LW}^{Lout,acet} - f_{PA-LW}^{Lin} x_{PA-LW}^{Lin,acet} - y_{PA-LW} \mathbf{U} \leq 0,$$

where \mathbf{U} is a large positive number.

To aid structural optimization and to introduce capital cost considerations, binary variables are employed to model block interconnections, for example, the existence of a flow from the lean outlet of the PA-LP block to the cold inlet of the

LP-LW exchanger. Such variables are not necessary; however, they simplify the solution of intermediate nonlinear program (NLP) subproblems through bounds of the type:

$$f - w \mathbf{U} \leq 0,$$

where f is an interconnection flow and w the corresponding binary variable.

Solution of large mixed integer linear programming (MILP) subproblems is aided with logical constraints of the type

$$w - y \leq 0,$$

that is, if a block does not exist, the corresponding interconnections cannot exist either.

Any air-liquid mass-transfer block is sized as an absorption tower and the Kremser equation (Douglas, 1988) is employed:

$$N_{ij} = \frac{\ln \left[\left(1 - \frac{m_{ijc} f_{ij}^R}{f_{ij}^L} \right) \frac{(x_{ij}^{Rin,c} - m_{ijc} x_{ij}^{Lin,c} - b_{ijc})}{(x_{ij}^{Rout,c} - m_{ijc} x_{ij}^{Lin,c} - b_{ijc})} + \frac{m_{ijc} f_{ij}^R}{f_{ij}^L} \right]}{\ln \left(\frac{m_{ijc} f_{ij}^R}{f_{ij}^L} \right)},$$

where N_{ij} is the number of absorption trays corresponding to the mass/heat-exchange match between (i, j) ; f_{ij}^R and f_{ij}^L are average flow rates of the rich and the lean sides, respectively; $x_{ij}^{Rin,c}$, $x_{ij}^{Rout,c}$, $x_{ij}^{Lin,c}$ are inlet and outlet compositions of the transferred component c , accordingly, and m_{ijc} and b_{ijc} are constants that govern the mass transfer.

The arrangement of two liquid-vapor mass-transfer blocks, connected countercurrently at the lean and the rich sides, which is identified through integer constraints on decision/structural variables accounting for block interconnections, is sized as a conventional distillation column, based on Fenske and Underwood equations, with the simplifying assumptions of:

$$N = 2N_{\min}$$

$$R = 1.2R_{\min},$$

where N is the number of trays; N_{\min} is the minimum number of trays; R is the reflux ratio; and R_{\min} is the minimum reflux ratio, calculated from

$$N_{\min} = \frac{\ln \left[\left(\frac{x_{\text{top}}^{Lin,acet}}{(1 - x_{\text{top}}^{Lin,acet})} \right) \left(\frac{x_{\text{bottom}}^{Rout,acet}}{(1 - x_{\text{bottom}}^{Rout,acet})} \right) \right]}{\ln \alpha},$$

where $x_{\text{top}}^{Lin,acet}$, $x_{\text{bottom}}^{Rout,acet}$ account for top and bottom acetone compositions at the column and α for relative volatility;

$$R_{\min} = \left(\frac{1}{\alpha - 1} \right) \left[\frac{x_{\text{top}}^{Lin,acet}}{x_f^{acet}} - \frac{\alpha(1 - x_{\text{top}}^{Lin,acet})}{1 - x_f^{acet}} \right],$$

where x_f^{acet} is the feed acetone composition.

The resulting MINLP model features 848 rows, 544 continuous variables, and 127 binary variables. Sixteen out of 127 binary variables correspond to the existence of mass/heat-exchange blocks (Figure 9) and are actually necessary.

The model was solved using GBD through the modeling system GAMS. Starting from the structure illustrated in Figure 11, the solution was obtained in six GBD iterations.

Appendix B: Mass/Heat-Exchange Superstructure Model for Ethylene Glycol Example

The mass/heat-exchange superstructure in the ethylene glycol example involves 20 mass/heat-exchange blocks and associated heaters and coolers (see Figure 13). Thus, the superstructure model is greatly simplified in terms of interconnections, since each heat exchanger is associated to the inlet or the outlet of a mass/heat-exchanger side. The synthesis model involves:

Mass balances for total flows

- At initial splitters of existing streams, for example, at the initial splitter of $V(\text{EO}, \text{W}, \text{EG}, \text{DG})$:

$$F_{V(\text{EO}, \text{W}, \text{EG}, \text{DG})} = \sum_{L-L} f_{L-L}^{\text{CbrI}, V} + \sum_{V-L} (f_{V-L}^{\text{RI}, V} + f_{V-L}^{\text{CbrI}, V} + f_{V-L}^{\text{HbrI}, V}) + F_{V(\text{EO}, \text{W}, \text{EG}, \text{DG})}^{\text{tot}, \text{out}}$$

- Note that existing $V(\text{EO}, \text{W}, \text{EG}, \text{DG})$ corresponds to pure EO (raw material), available at the gas phase. Thus, it can only be fed to vapor-phase mixers, as coolers/condensers prior to rich-liquid side of $L-L$ blocks, vapor-rich side of $V-L$ blocks, and their corresponding coolers and heaters. For existing $L(\text{EO}, \text{W}, \text{EG}, \text{DG})$, corresponding to pure W feed, we have

$$F_{L(\text{EO}, \text{W}, \text{EG}, \text{DG})}^{\text{tot}, \text{in}} = \sum_{L-L} (f_{L-L}^{\text{RI}, L} + f_{L-L}^{\text{HbrI}, L}) + \sum_{V-L} (f_{V-L}^{\text{LI}, L} + f_{V-L}^{\text{CbII}, L} + f_{V-L}^{\text{HbII}, L}) + F_{L(\text{EO}, \text{W}, \text{EG}, \text{DG})}^{\text{out}, L}$$

Note that in the $L-L$ blocks, we have only rich inlets.

- At stream splitters at the outlet of each exchanger block, that is,
 - mass/heat-exchange blocks, with stream flows going to final stream outlets or other exchanger block inlets (mass/heat or pure heat). Note that in $L-L$ blocks we have only one lean outlet; for example, at the lean outlet of an $L-L$ block

$$f_{L-L}^{\text{out}} = \sum_{L-L} (f_{L-L}^{\text{LRB}, L-L} + f_{L-L}^{\text{LHbrB}, L-L}) + \sum_{V-L} (f_{V-L}^{\text{LLB}, L-L} + f_{V-L}^{\text{LHbIB}, L-L} + f_{V-L}^{\text{LCbIB}, L-L}) + f_{L-L}^{\text{HalB}, L-L} + f_{L-L}^{\text{CalB}, L-L} + F_{L(\text{EO}, \text{W}, \text{EG}, \text{DG})}^{\text{out}, L-L} + F_{L(\text{EG})}^{\text{out}, L-L} + F_{L(\text{DG})}^{\text{out}, L-L}$$

- heat-exchange blocks associated with inlets of mass/heat-exchange blocks, where the outlet flow is, for example, forwarded toward the following exchanger.

- heat-exchange blocks associated with outlets of mass/heat-exchange blocks, similar to mass/heat exchangers.

- at stream mixers at the inlets of each exchanger, for example, at the lean inlet of a $V-L$ blocks.

$$f_{V-L}^{\text{LI}, \text{in}} = \sum_{L-L} (f_{L-L}^{\text{LLB}, L-L} + f_{L-L}^{\text{LHalB}, L-L} + f_{L-L}^{\text{LCalB}, L-L}) + \sum_{V-L} (f_{V-L}^{\text{LLB}, V-L} + f_{V-L}^{\text{LHalB}, V-L} + f_{V-L}^{\text{LCalB}, V-L}) + f_{V-L}^{\text{LHbIB}, V-L} + f_{V-L}^{\text{LCbIB}, V-L} + f_{V-L}^{\text{LI}, L}$$

- At final stream mixers.

Component mass balances

- At the mixers and splitters of the superstructure, similar to total flows

- At heat exchangers, where no change in stream composition takes place

- At mass/heat exchangers, where we account for mass exchange due to reaction and phase change, for example, at the lean side of a $V-L$ exchanger and for EG:

$$f_{V-L}^{\text{in}} c_{V-L}^{\text{in}, \text{EG}} - f_{V-L}^{\text{out}} c_{V-L}^{\text{out}, \text{EG}} + M_{V-L}^{\text{react}, \text{EG}} + M_{V-L}^{\text{trans}, \text{EG}} = 0,$$

where

$$M_{V-L}^{\text{react}, \text{EG}} = (k_{V-L}^{\text{r1}} c_{V-L}^{\text{out}, \text{EO}} c_{V-L}^{\text{out}, \text{W}} - k_{V-L}^{\text{r2}} c_{V-L}^{\text{out}, \text{EO}} c_{V-L}^{\text{out}, \text{EG}}) V_{L-V-L}$$

Table 8 illustrates the type and number of equations and variables that describe an $L-V$ module.

Summation of molar fractions to 1.

Enthalpy balances

- At the mixers of the superstructure, similar to component mass balances

- At heat-exchange blocks, for example, at a heater before the lean side of a $V-L$ exchanger

$$f_{V-L}^{\text{HbI}, \text{in}} \sum_i (c_{V-L}^{\text{HbI}, \text{in}, i} h_{V-L}^{\text{HbI}, \text{in}, i}) - f_{V-L}^{\text{HbI}, \text{out}} \sum_i (c_{V-L}^{\text{HbI}, \text{out}, i} h_{V-L}^{\text{HbI}, \text{out}, i}) = Q_{V-L}^{\text{HbI}}$$

- At mass/heat-exchange blocks accounting for reaction and phase-change enthalpy, for example, at a $V-L$ exchanger

$$f_{V-L}^{\text{Rin}} \sum_i (c_{V-L}^{\text{Rin}, i} h_{V-L}^{\text{Rin}, i}) + f_{V-L}^{\text{Lin}} \sum_i (c_{V-L}^{\text{Lin}, i} h_{V-L}^{\text{Lin}, i}) - f_{V-L}^{\text{Rout}} \sum_i (c_{V-L}^{\text{Rout}, i} h_{V-L}^{\text{Rout}, i}) - f_{V-L}^{\text{Lout}} \sum_i (c_{V-L}^{\text{Lout}, i} h_{V-L}^{\text{Lout}, i}) + QR_{V-L} = 0,$$

where

$$QR_{V-L} = (k_{V-L}^{\text{r1}} c_{V-L}^{\text{out}, \text{EO}} c_{V-L}^{\text{out}, \text{W}} DH_{V-L}^{\text{r1}} + k_{V-L}^{\text{r2}} c_{V-L}^{\text{out}, \text{EO}} DH_{V-L}^{\text{r2}}) V_{L-V-L}$$

- At final stream mixers

Phase-defining constraints, as in the acetone recovery example (Appendix A).

Driving force constraints for EG mass transfer at mass/heat-exchange blocks, for example, $L-L$ exchangers, mass transfer is based on reaction, and the driving force will be

$$k_{L-L}^{r1} c_{L-L}^{Lout,EO} c_{L-L}^{Lout,W} - k_{L-L}^{r2} c_{L-L}^{Lout,EO} c_{L-L}^{Lout,EG} \geq 0$$

at $V-L$ exchangers, mass transfer is based on phase change:

$$c_{V-L}^{Lout,EG} - \frac{1}{k_{V-L}^{Lout,EG}} c_{V-L}^{Rin,EG} \leq 0.$$

Driving-force constraints for heat exchange at heaters and coolers.

The existence of each mass/heat and pure heat-transfer block is denoted by a binary variable and defined by mixed-integer constraints of the type (Appendix A):

$$M^{\text{exchange}} - yU \leq 0,$$

where M^{exchange} for $L-L$ matches is the reacted mass, while in $V-L$ matches are based on phase change, since the reaction takes place in the liquid phase.

Manuscript received Feb. 23, 1995, and revision received May 23, 1995.

Corrections

The article titled "Studies of Aggregation Effects on SO_x Removal by Limestone Powder" by Yoshio Kobayashi (December 1995, p. 2642) has 32 pages of supplementary material. The material has been filed with NAPS (file no. 05284) and can be purchased from NAPS, Microfiche Publications, P.O. Box 3513, Grand Central Station, New York, NY 10163. NAPS requires advance remittance of \$11.35 for photocopies or \$4.00 for microfiche in U.S. funds only. There is a \$15.00 invoicing charge on all orders filled before payment. Outside U.S. and Canada, add mailing charge of \$4.50 for the first 20 pages and \$1.00 for each ten pages of material thereafter, or \$1.75 for the first microfiche and \$0.50 for each fiche thereafter.

In addition, the following corrections and addition to the above article are made.

- The sentence immediately before Eq. A3 (p. 2652) should read "From Eqs. A1 and A2, Eq. A3 can be obtained," not "From Eqs. A1 to A3 can be obtained."
- The last line of the third paragraph on the righthand column of p. 2650 should read "83% of the reaction," instead of "86% of the reaction."
- The current address of Y. Kobayashi is 16-22 Jiyugaoka 2-chrome, Kumatori-cho, Osaka 590-04, Japan.

In the article titled "Wave Model for Longitudinal Dispersion: Analysis and Applications" by K. R. Westerterp et al. (September 1995, p. 2029), the following corrections are made:

Equation 33 on p. 2035 should be changed to

$$\sigma_t^2 = \sigma_{t,0}^2 + 2 \left(\frac{x}{u} \right)^2 \frac{D_e}{xu} [\lambda(1 + 2u_a^* - 3D_e^*) + \left[-\lambda(u_a^* - 2D_e^*) + \frac{3D_e^* - 1 - 2u_a^*}{\zeta} \right] (1 - e^{-\lambda\zeta}) - \frac{D_e^*}{2\zeta} (1 - e^{-\lambda\zeta})^2] \quad (33)$$

In the limiting cases of $\zeta \gg 1$ and $\zeta \ll 1$, this equation takes the forms:

$$\sigma_t^2 = \sigma_{t,0}^2 + 2 \left(\frac{x}{u} \right)^2 \frac{D_e}{xu} \left[1 + \frac{5 D_e}{2 ux} - \frac{u\tau}{x} \left(1 + \frac{2u_a}{u} \right) \right]$$

$$\sigma_t^2 = \sigma_{t,0}^2 + \left(\frac{x}{u} \right)^2 \frac{D_e u^2 \tau}{[u(u + u_a)\tau - D_e]^2}$$

Equation 46 on p. 2037 should be changed to

$$\Delta t = \tau \ln(2e^{t_R/\tau} - 1) - t_R$$